

UNIEDIT-FLOW: Unleashing Inversion and Editing in the Era of Flow Models

Guanlong Jiao
Tsinghua University
jgl22@mails.tsinghua.edu.cn

Biqing Huang
Tsinghua University
hbq@tsinghua.edu.cn

Kuan-Chieh Wang
Snap Inc.
jwang23@snapchat.com

Renjie Liao
The University of British Columbia
renjie.liao@ubc.ca

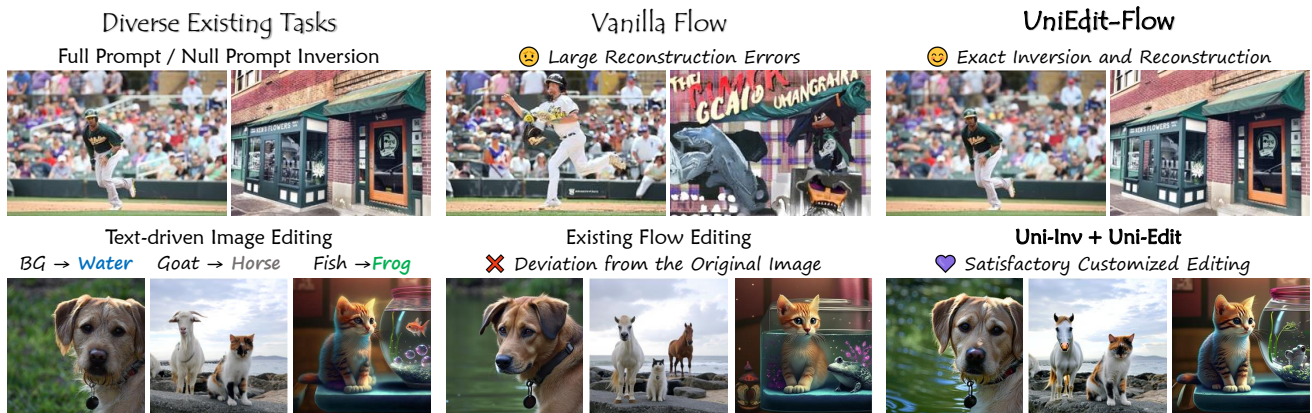


Figure 1. **UniEdit-Flow for image inversion and editing.** Our approach proposes a *highly accurate and efficient, model-agnostic, training and tuning-free* sampling strategy for flow models to tackle image inversion and editing problems. Cluttered scenes are difficult for inversion and reconstruction, leading to failure results on various methods. Our Uni-Inv achieves **exact reconstruction** even in such complex situations (1st line). Furthermore, existing flow editing always maintain undesirable affects, out region-aware sampling-based Uni-Edit showcases excellent performance for **both editing and background preservation** (2nd line).

Abstract

Flow matching models have emerged as a strong alternative to diffusion models, but existing inversion and editing methods designed for diffusion are often ineffective or inapplicable to them. The straight-line, non-crossing trajectories of flow models pose challenges for diffusion-based approaches but also open avenues for novel solutions. In this paper, we introduce a predictor-corrector-based framework for inversion and editing in flow models. First, we propose Uni-Inv, an effective inversion method designed for accurate reconstruction. Building on this, we extend the concept of delayed injection to flow models and introduce Uni-Edit, a region-aware, robust image editing approach. Our methodology is tuning-free, model-agnostic, efficient, and effective, enabling diverse edits while ensuring strong preservation of edit-irrelevant regions. Extensive experiments across vari-

ous generative models demonstrate the superiority and generalizability of Uni-Inv and Uni-Edit, even under low-cost settings. Project page: <https://uniedit-flow.github.io/>.

1. Introduction

Diffusion models have revolutionized the field of image generation and created well-known text-to-image foundation models [26, 43, 49, 51]. They have also enabled a suite of applications ranging from personalized image generation [20, 53, 70, 81], image editing [2, 3, 6, 86], using image models as a prior for 3D generation [46, 50, 62, 82], to even non-generative tasks [17, 34, 54, 83]. Among these, the application of real image editing uniquely leverages the fact that diffusion models learn a mapping between the prior (noise) distribution and the distribution of real im-

ages. By simply adding noise to a real-image, which mimicks the training process, and performing denoising with a new condition (e.g. a modified prompt), a pre-trained diffusion model can be naturally repurposed to an image editor. This has led to a multitude of *inversion* methods [38, 58, 60, 66, 67], and a myriad of *training-free, inversion-based* image editing methods [2, 5, 7, 14, 23, 47].

Recently, a new class of models similar to diffusion models known as *flow* models have gained favor and dominated text-to-image tasks such as Stable Diffusion 3 (SD3) [19] and Flux [33]. These models differ from the the previous generation of models based on diffusion in two key aspects:

1. *Formulation Change* – Flow models are based on deterministic probability flow ordinary differential equations (PF-ODEs), in contrast to diffusion models which are based on SDEs. More specifically, SD3 and Flux uses the rectified flow formulation which models straight lines between the two distributions.
2. *Architecture Change* – In conjunction, there was a shift in architecture from U-Nets with cross-/self-attention layers to using DiTs [43] and MM-DiTs [19] to improve their *data scaling* ability.

As a result, many methods effective in diffusion models face challenges when applied to flow models. To bridge this gap, recent works have introduced specialized modifications to joint attention in MM-DiTs [4, 15, 69, 80]. Meanwhile, other approaches attempt to reintroduce stochasticity into flow models [52, 57, 68], effectively aligning them with diffusion models. However, many of these methods ultimately retrace the trajectory of diffusion models, raising questions about their differences with respect to diffusion and long-term impact.

Our paper aims to re-design inversion and editing by explicitly accounting for the two design changes in the foundation model. We first examine the diffusion-based techniques that fail to transfer effectively to flow models, analyzing their behavior across different architectures. Specifically, we investigate the degradation of the so-called “delayed injection” in flow models, along with the impact of trajectory properties—where vanilla inversion leads to localized sampling errors, as shown in Fig. 1. We argue that the straight-line and non-crossing trajectories of flow models make them prone to accumulating significant errors and even collapsing when velocity estimation is inaccurate during inversion and reconstruction. Furthermore, these properties complicate conditional trajectory guidance, posing challenges for tuning-free editing. Despite these difficulties, we focus on leveraging these characteristics strategically, aiming to unlock the unexplored potential of flow models.

We introduce a novel predictor-corrector-based inversion method for flow models, aiming for accurate and stable reconstruction. Furthermore, we propose a robust sampling-

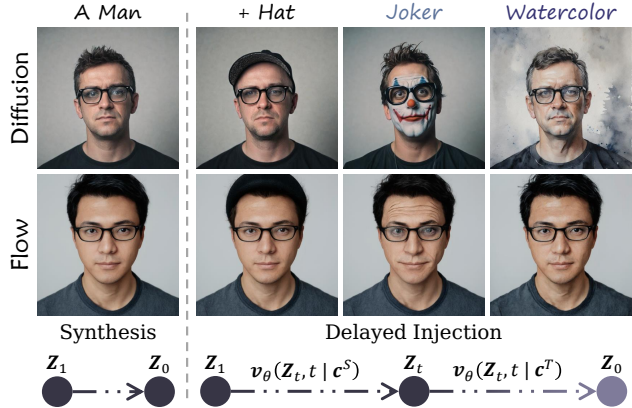


Figure 2. **Delayed injection**, which retains the source condition during the early denoising steps and introduces the edit condition at a middle timestep (illustrated in the bottom part), is a widely used technique in diffusion-based editing (top row). However, when applied to flow models (second row), it is ineffective. While flow-based editing exhibits a mild tendency toward the target edit, it fails to produce sufficiently strong effects.

based editing strategy with region-adaptive guidance and velocity fusion, enabling effective and interpretable text-driven image editing. Through both theoretical and empirical analyses, we validate our approach on several benchmarks and demonstrate state-of-the-art performance across diverse generative models, including flow models (Stable Diffusion 3 [19] and FLUX [33]) as well as diffusion models (results in Appendix E).

2. Related Work

Inversion. Modern generative models, particularly diffusion models, aim to map a standard Gaussian distribution to the real data distribution [22, 26]. Inversion, the reverse of the generation process, seeks to recover the latent noise corresponding to a given image by reconstructing the diffusion trajectory [58, 66]. The introduction of DDIM [58] marked a significant step forward, inspiring a series of high-precision solvers designed to enhance sampling efficiency and minimize inversion errors [38, 38, 67, 85]. To further improve alignment between input images and their reconstructions from inverted noise, tuning-based methods have been developed to mitigate reconstruction bias [21, 30, 40, 65]. More recently, the emergence of flow models has driven the adoption of deterministic samplers, introducing alternative approaches to inversion [16, 52, 57, 59, 69]. These methods design sampling strategies to reduce discretization errors in inversion. However, their non-reconstruction-oriented designs and restrictions on sampler selection limit their applicability to inversion-based tasks such as image editing. In this work, we focus on the inversion and reconstruction process, designing UniInv to achieve high reconstruction reliability and local ex-

actness, making it well-suited for downstream applications. **Text-driven Image Editing.** For image editing tasks, early training-based approaches explored generative models to achieve controllable modifications [31, 89]. With the advancement of generative models, the focus has shifted toward training-free editing methods, which offer greater flexibility and efficiency. Tuning-based methods have demonstrated impressive results but require iterative optimization during generation, leading to increased computational costs [18, 30, 41, 76]. Meanwhile, attention-manipulation-based techniques leverage multi-branch frameworks for precise control, but their applicability is often restricted to specific model architectures [11, 79]. Sampling-based methods introduce controlled randomness or guidance mechanisms to achieve more flexible editing [8, 27, 63, 71]. More recently, the rise of flow models built on MM-DiT [19] has attracted significant attention in the editing domain due to their strong generative capabilities [37, 39, 42, 61]. In this work, we rethink the design of efficient and generalizable image editing methods in the era of flow models, introducing Uni-Edit, a model-agnostic and adaptable approach tailored for text-driven image editing tasks.

3. Background

3.1. Flow Matching

Generative models aim at generating data that follows the real data distribution π_0 from noise that follows some known distribution π_1 (e.g., Gaussian distribution). Flow matching [1, 35, 36] proposed to learn a velocity field that is parameterized by a neural network to move noise to data via straight trajectories. The training objective is to solve the following optimization problem:

$$\min_{\theta} \mathbb{E}_{\mathbf{Z}_0, \mathbf{Z}_1, t} \left[\|\mathbf{Z}_1 - \mathbf{Z}_0 - \mathbf{v}_{\theta}(\mathbf{Z}_t, t)\|^2 \right], \quad (1)$$

$$\mathbf{Z}_t = t\mathbf{Z}_1 + (1-t)\mathbf{Z}_0, t \in [0, 1],$$

where data $\mathbf{Z}_0 \in \pi_0$ and noise $\mathbf{Z}_1 \in \pi_1$. $\mathbf{Z}_1 - \mathbf{Z}_0$ is the target velocity and $\mathbf{v}_{\theta}(\cdot)$ is the learnable velocity field. The trained model is expected to estimate a velocity field to map a randomly sampled Gaussian noise $\mathbf{Z}_1 \in \mathcal{N}(0, \mathbf{I})$ to generated data \mathbf{Z}_0 in a deterministic way. This generation process can be viewed as solving an ordinary differentiable equation (ODE) characterized by $d\mathbf{Z}_t = \mathbf{v}_{\theta}(\mathbf{Z}_t, t) dt$. This ODE can be discretized and then numerically solved by solvers such as the Euler method:

$$\mathbf{Z}_{t_{i-1}} = \mathbf{Z}_{t_i} + (t_{i-1} - t_i) \mathbf{v}_{\theta}(\mathbf{Z}_{t_i}, t_i), \quad (2)$$

where $i \in \{N, \dots, 0\}$, $t_N = 1$, and $t_0 = 0$.

3.2. Delayed Injection

Previous works have introduced delayed injection, a simple yet effective technique that helps maintain image consistency during editing. This method preserves the original

conditions or reuses the latent representations from the inversion process before a specific timestep while injecting the editing conditions afterward, enabling a balanced trade-off between content preservation and targeted modifications [14, 75, 78]. As illustrated in Fig. 2, the top row demonstrates a diffusion-based example, where delayed injection enables an effective trade-off between preserving editing-irrelevant content and achieving the intended editing. Due to the non-linear and intersecting sampling trajectories of diffusion models, modifying conditions midway allows for trajectory transitions, facilitating more flexible and localized image editing [42]. However, flow models exhibit straight-line and non-intersecting trajectories [36], which fundamentally hinder the effectiveness of delayed injection, particularly in image editing. As shown in the middle of Fig. 2, applying delayed injection under similar conditions leads to limited improvements in flow-based editing. In this work, we take a deeper look into how to design effective guidance strategies for delayed injection, aiming to unlock more controllable and reliable flow-based image editing.

4. Method

Fig. 3 provides a brief illustration of image inversion, reconstruction, and editing based on vanilla ODE sampling methods, as well as an overview of our approach. In Fig. 3 (a), due to the mismatch between \mathbf{Z} and t used in each corresponding forward step, it's difficult for direct inversion to ensure consistency between the reconstructed image and the original one. Besides, conditional denoising without proper guidance cannot enable controllable image editing and leads to undesirable results. In Fig. 3 (b), we implement the idea of predictor-corrector in two distinct forms for inversion and editing, respectively. In this section, we will first present our proposed Uni-Inv and Uni-Edit for inversion and editing, respectively. We will then introduce other technical contributions, such as region-adaptive guidance and velocity fusion.

4.1. Uni-Inv

The motivation of Uni-Inv is to conduct an accurate inversion capable of inverting ODE solutions back to the initial value for particular deterministic samplers. We take the flow model [19, 36] with an Euler method solver as a simple instance of deterministic iterative generation methods facilitated by its concise formula. Eq. (2) describes one iteration step in which we estimate $\mathbf{Z}_{t_{i-1}}$ from \mathbf{Z}_{t_i} by a denoising step. Through this formulation, we can derive the exact value of the inverted latent \mathbf{Z}_{t_i} :

$$\mathbf{Z}_{t_i} = \mathbf{Z}_{t_{i-1}} - (t_{i-1} - t_i) \mathbf{v}_{\theta}(\mathbf{Z}_{t_i}, t_i). \quad (3)$$

However, in the inversion process, since there is no access to \mathbf{Z}_{t_i} , $\mathbf{v}_{\theta}(\mathbf{Z}_{t_i}, t_i)$ in Eq. (3) is unknown. Previous tuning-free approaches replace $\mathbf{v}_{\theta}(\mathbf{Z}_{t_i}, t_i)$ with an approximation,

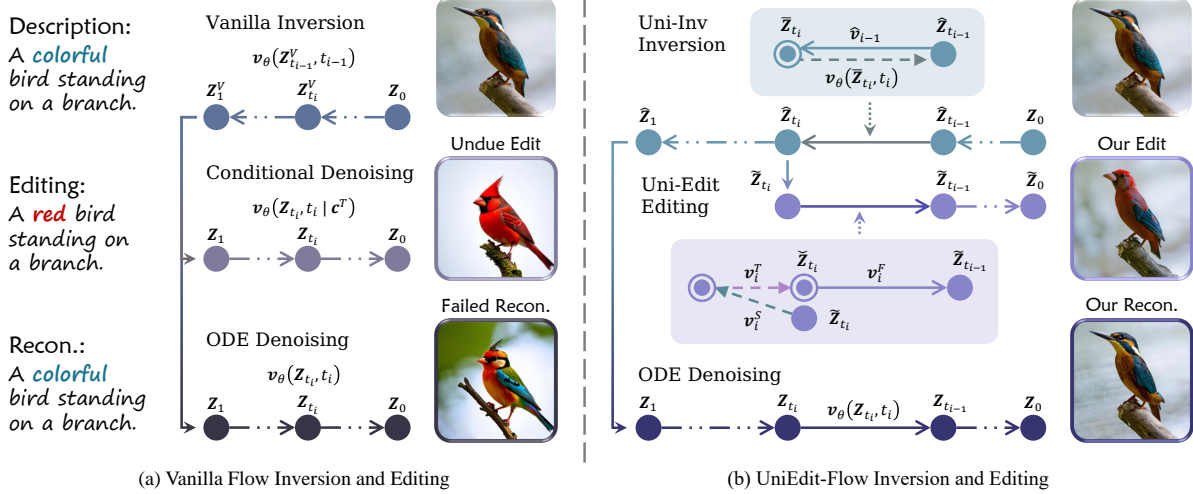


Figure 3. **An overview** of our proposed Uni-Inv and Uni-Edit (bird \rightarrow red bird). (a) indicates that vanilla flow inversion is incapable for both exact image inversion and controllable editing. (b) demonstrates our proposed Uni-Inv and Uni-Edit, which perform efficient and effective inversion and editing.

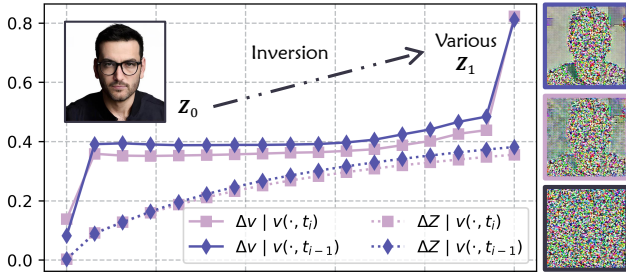


Figure 4. **Per-step error of the velocities and samples** of vanilla inversions. We first synthesis an image Z_0 , then conduct vanilla inversion to get inverted noises Z_1 with per-step velocity of $v_\theta(\hat{Z}_{t_{i-1}}, t_{i-1})$ (\blacklozenge) and $v_\theta(\hat{Z}_{t_{i-1}}, t_i)$ (\blacksquare), respectively. We plot the per-step local error of samples (ΔZ) velocities (Δv). The right shows the visualization of various Z_1 , while their border colors correspond to different conditions (black for the initial noise).

e.g., $v_\theta(Z_{t_{i-1}}, t_{i-1})$ in DDIM Inversion [58, 60]. Such an approximation assumes that model predictions are consistent across timesteps, which is bound to have errors. Empirically, we find in the inversion steps, evaluating $v_\theta(\hat{Z}_{t_{i-1}}, \cdot)$ at t_i , which corresponds to the local target of the inversion step $\hat{Z}_{t_{i-1}}$, yields more accurate velocities compared to evaluating it at t_{i-1} . As shown in Fig. 4, $v_\theta(\hat{Z}_{t_{i-1}}, t_{i-1})$ (\blacklozenge) constantly achieves a larger local error compared to $v_\theta(\hat{Z}_{t_{i-1}}, t_i)$ (\blacksquare), and ultimately it reconstructs a different noise with a mismatched background. Since t_i is accessible, we can evaluate the velocity at this point in the inversion for better reconstruction. Notably, the error accumulation of both vanilla strategies is non-trivial, as inaccurate velocity estimates continually deviate from the original trajectory. Therefore, the key to effective image inversion and reconstruction lies in finding a \tilde{Z}_{t_i} via $\hat{Z}_{t_{i-1}}$ to align the

Algorithm 1 Uni-Inv (Euler)

Input:

Velocity Function v_θ , Initial Image $Z_0 \sim \pi_0$,
Time Steps $t = \{t_0, \dots, t_N\}$, $t_0 = 0$, $t_N = 1$.

Initial:

$\hat{v}_0 \leftarrow v_\theta(Z_0, t_0)$
 $\hat{Z}_{t_0} \leftarrow Z_0$

For $i = 1$ to N do

- 1: $\tilde{Z}_{t_i} \leftarrow \hat{Z}_{t_{i-1}} - (t_{i-1} - t_i)\hat{v}_{i-1}$ \triangleright Correction
- 2: $\hat{v}_i \leftarrow v_\theta(\tilde{Z}_{t_i}, t_i)$ \triangleright Prediction
- 3: $\hat{Z}_{t_i} \leftarrow \hat{Z}_{t_{i-1}} - (t_{i-1} - t_i)\hat{v}_i$ \triangleright Sample Update

End for

Output: \hat{Z}_1

velocity fields at time t_i and t_{i-1} .

To estimate a proper \tilde{Z}_{t_i} , methods like ReNoise [21] suggest utilizing recursive sampling, but this approach significantly increases computational cost. Inspired by the straight trajectories of Rectified Flow [36], we propose reusing the previously obtained velocity \hat{v}_{i-1} at the current time step to avoid extra model evaluations. We first use this velocity to backtrack the sample from t_{i-1} to t_i , thereby correcting intermediate inversion steps. Then, for the next inversion step, we compute a velocity \hat{v}_i that is better aligned with step t_i .

Alg. 1 provides an overview of Uni-Inv. Intuitively, Uni-Inv introduces a correction procedure before performing the inversion step. It first transitions to the high-noise step and estimates the velocity by simulating a denoising procedure. Then it returns to the original low-noise step and performs inversion using the latest “denoising-like” velocity.

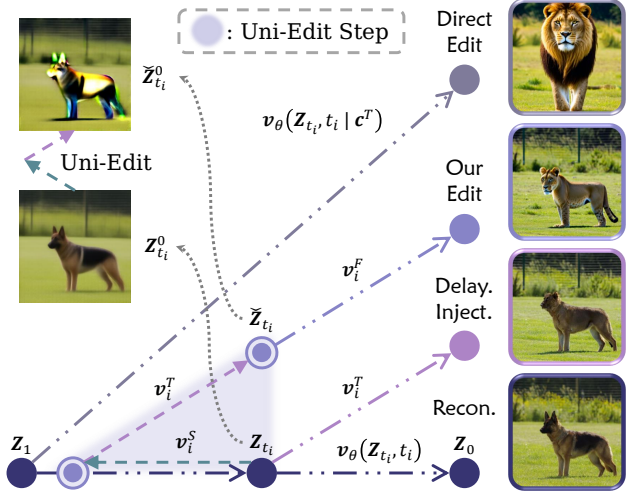


Figure 5. **Demonstration of various sampling-based image editing methods** (dog \rightarrow lion). Directly utilizing c^T as condition leads to an undue editing. Leveraging delayed injection, which is widely used in diffusion-based methods, inevitably results in an inchoate performance when using deterministic models. Our Uni-Edit mitigates early steps obtained components that are not conducive to editing, ultimately achieving satisfying results.

Proposition 4.1. *Suppose the velocity field v_θ is Lipschitz, and there is a constant C such that $\|\mathbf{Z}_{t_p} - \mathbf{Z}_{t_q}\| \leq C \|t_p - t_q\|, \forall t_p, t_q \in [0, 1]$, where \mathbf{Z}_{t_p} and \mathbf{Z}_{t_q} come from the same sampling process. Then for any two consecutive steps t_{i-1} and t_i , the local error of inversion and reconstruction using Uni-Inv is $\mathcal{O}(\Delta t_i^3)$, where $\Delta t_i = t_i - t_{i-1}$.*

This result provides the local error, *i.e.*, the one-step error for inversion and reconstruction. It gives the theoretical guarantee for the quality of Uni-Inv for reconstruction. We provide the proof of Prop. 4.1 in Appendix A.

4.2. Uni-Edit

Sec. 3.2 provides a case study that highlights the challenges faced by flow models in image editing tasks. As shown in Fig. 5, delayed injection aims to establish an intermediate state between the original and editing trajectories. However, due to the non-intersecting nature of flow trajectories, it is difficult to obtain significantly different directions from middle steps, often resulting in **inchoate results**. On the other hand, unrestricted direct sampling with editing conditions often leads to **undesirable edit**, as the generated sample diverges from the original trajectory from the outset. To address these issues, an intuitive strategy is to inject editing conditions earlier while mitigating excessive modifications using information from the current latent state. Instead of simply injecting conditions earlier, we propose additional correction steps during the editing procedure solely based on the current latent $\tilde{\mathbf{Z}}_{t_i}$. At the injection step, this variable is initialized as the inversion latent, *i.e.*, $\tilde{\mathbf{Z}}_{t_{\alpha N}} = \hat{\mathbf{Z}}_{t_{\alpha N}}$,

Algorithm 2 Uni-Edit (Euler)

Input:

Velocity Function v_θ , Initial Image $\mathbf{Z}_0 \sim \pi_0$,
 Source Condition c^S , Target Condition c^T ,
 Guidance Strength ω , Delay Rate α ,
 Time Steps $t = \{t_0, \dots, t_{\alpha N}\}$, $t_0 = 0$, $t_{\alpha N} \leq 1$.

Initial:

$\tilde{\mathbf{Z}}_{t_{\alpha N}} \leftarrow \text{Uni-Inv}(v_\theta, \mathbf{Z}_0, t)$
 $\tilde{\mathbf{Z}}_{t_{\alpha N}} \leftarrow \tilde{\mathbf{Z}}_{t_{\alpha N}}$

For $i = \alpha N$ to 1 do

- 1: $v_i^S, v_i^T \leftarrow v_\theta(\tilde{\mathbf{Z}}_{t_i}, t_i | c^S), v_\theta(\tilde{\mathbf{Z}}_{t_i}, t_i | c^T)$ \triangleright Prediction
- 2: $v_i^- \leftarrow v_i^T - v_i^S$ \triangleright Velocity Difference
- 3: $m_i \leftarrow \text{Mask}(v_i^-)$ \triangleright Guidance Mask
- 4: $s_i \leftarrow \omega(t_{i-1} - t_i)(1 + m_i) \odot v_i^-$ \triangleright Correction Stride
- 5: $\tilde{\mathbf{Z}}_{t_i} \leftarrow \tilde{\mathbf{Z}}_{t_i} + s_i$ \triangleright Correction
- 6: $v_i^F \leftarrow m_i \odot v_i^T + (1 - m_i) \odot v_i^S$ \triangleright Velocity Fusion
- 7: $\tilde{\mathbf{Z}}_{t_{i-1}} \leftarrow \tilde{\mathbf{Z}}_{t_i} + (t_{i-1} - t_i)v_i^F$ \triangleright Sample Update

End for

Output: $\tilde{\mathbf{Z}}_0$

where α denotes the delay rate and N is the total number of sampling steps. As shown in Fig. 3 and 5, given a source condition c^S that describes the source image and a target condition c^T that specifies the editing objective, we compute two different velocity estimates, v_i^S and v_i^T , via the velocity field v_θ . To introduce a correction step, $\tilde{\mathbf{Z}}_{t_i}$ is first transitioned to a previous step with higher noise along the direction of v_i^S . It is then mapped back to $\tilde{\mathbf{Z}}_{t_i}$ via v_i^T , which is aligned with the current timestep t_i . This predictor-corrector procedure corrects undesirable components introduced in early sampling steps that may hinder effective editing. Finally, we apply the current editing velocity to move the latent to $\tilde{\mathbf{Z}}_{t_{i-1}}$, achieving a **proper edit**.

4.3. Region-Adaptive Guidance and Velocity Fusion

Previous works have observed that the difference between latents conditioned on different prompts highlights regions crucial for editing [14, 24]. Building on this insight, we leverage this difference v_i^- to construct a mask $m_i = \text{Mask}(v_i^-)$, which serves as regional guidance for correction and velocity prediction, thereby improving the controllability of Uni-Edit. Here, $\text{Mask}(\cdot)$ denotes the min-max normalization of the channel-wise mean map. To guide the inversion process, we first apply a weighting factor of $(1 + m_i)$, encouraging edit-relevant regions to backtrack with a larger stride, thereby enhancing the removal of original concepts crucial for the intended modification. For the subsequent sample update, we fuse the target and source velocities, v_i^T and v_i^S , using m_i and $(1 - m_i)$ as respective weights. This ensures that edit-irrelevant regions remain largely unmodified, preventing excessive alterations.

The complete editing procedure is outlined in Alg. 2. The delayed injection framework, parameterized by the de-

Method	Model	Unconditional				Conditional			
		MSE \downarrow_{10^3}	PSNR \uparrow	SSIM \uparrow_{10^2}	LPIPS \downarrow_{10^2}	MSE \downarrow_{10^3}	PSNR \uparrow	SSIM \uparrow_{10^2}	LPIPS \downarrow_{10^2}
Euler	SD3	29.98	16.54	58.97	29.03	29.14	16.80	57.54	29.92
Heun		25.34	16.98	67.25	26.63	26.32	16.89	64.14	27.70
RF-Solver [69]		45.24	15.43	56.57	33.67	26.54	18.52	64.10	26.38
FireFlow [16]		<u>20.27</u>	<u>19.60</u>	<u>66.96</u>	<u>25.29</u>	16.95	<u>20.85</u>	68.89	<u>22.83</u>
Ours		11.52	21.81	78.89	12.85	7.86	23.41	82.23	9.53
Euler	FLUX	90.59	11.10	40.51	43.13	85.69	11.43	37.64	44.31
Heun		83.04	11.77	42.10	39.96	76.79	12.17	40.17	41.18
RF-Solver [69]		29.32	16.97	57.17	31.75	34.71	16.38	55.64	32.43
FireFlow [16]		<u>23.31</u>	<u>18.15</u>	<u>63.85</u>	<u>27.96</u>	<u>30.78</u>	<u>17.59</u>	<u>62.51</u>	<u>28.30</u>
Ours		8.85	22.15	79.45	17.10	14.36	20.91	77.09	20.27

Table 1. **Quantitative results for inversion and reconstruction.** For Stable Diffusion 3 (SD3) [19], we keep each method’s NFE close to 100, which means we set sampling step to 50 for once-forward methods (*i.e.*, Euler, FireFlow, and Ours) and to 25 for twice-forward methods (*i.e.*, Heun and RF-Solver). For FLUX [32], we keep NFE close to 60 (*i.e.*, 30 for once-forward methods and 15 steps for twice-forward methods). We adopt the official implementations of baselines for FLUX, and reimplement their methods for SD3. The best and second best results are **bolded** and underlined, respectively. Cells are highlighted from worse to better.

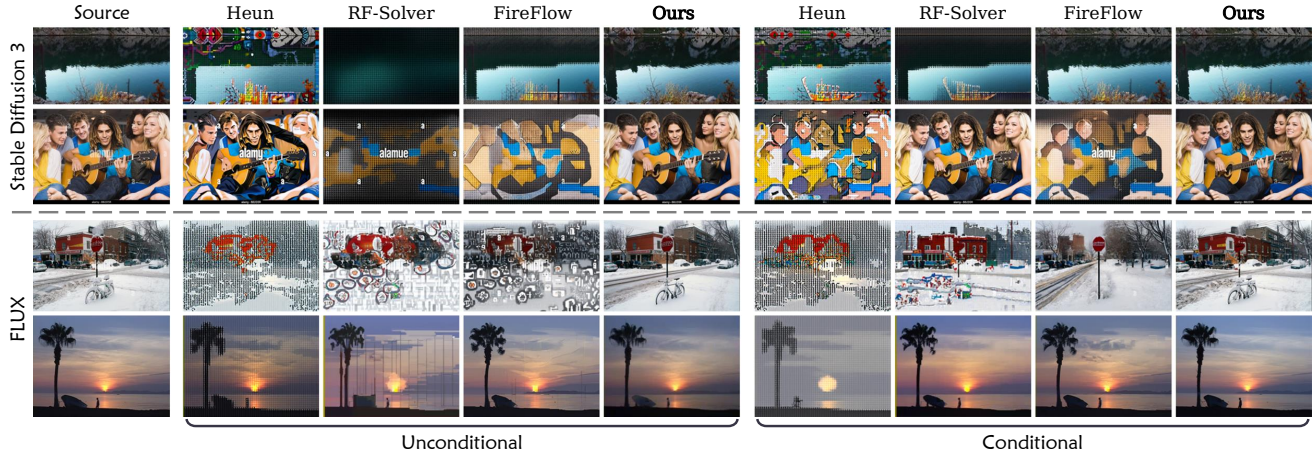


Figure 6. **Qualitative comparison on inversion & reconstruction.** Our method ensures stable reconstruction results in both situations with description accessible (conditional) and inaccessible (unconditional), while taking into account both overall and detail consistency.

lay rate α , strikes a balance between preserving background details and achieving effective modifications, while simultaneously reducing inference costs. By integrating regionally enhanced guidance with velocity fusion, we ultimately obtain an adaptive and computationally efficient editing approach. Furthermore, our velocity fusion method offers advantages over existing latent fusion techniques [14, 24] by providing better performance without additional memory overhead, as illustrated in Fig. 8. We further provide the theoretical analysis of Uni-Edit in Appendix B and details of our model variants in Appendix D.

5. Experiments

5.1. Setup

Baselines: We conduct experiments on two tasks: 1) image inversion and reconstruction; 2) text-driven image edit-

ing. For image inversion and reconstruction, we compare our Uni-Inv with the Euler and the Heun method, as well as flow-based methods like RF-Solver [69] and FireFlow [16]. For text-driven image editing, we compare our Uni-Edit with diffusion-based methods: P2P [25], PnP [65], PnP-Inversion [30], EditFriendly [27], MasaCtrl [11], and InfEdit [79], along with the aforementioned two flow-based methods. More tuning-based [21, 40] and training-based methods [10, 56, 74, 77] are discussed in Appendix E.

Benchmarks and Metrics: For inversion and reconstruction, we report the average MSE, PSNR [29], SSIM [72], and LPIPS [87] of reconstructed images on the Conceptual Captions validation dataset [55], which consists of 13.4K images annotated with captions. These metrics are evaluated in both conditional (using image captions as prompts) and unconditional (using null text only) settings. For text-driven image editing, we conduct experiments on PIE-

Method	Model	Structure	BG Preservation		CLIP Sim.↑		Steps	NFE
		Distance↓ _{10³}	PSNR↑	SSIM↑ _{10²}	Whole	Edited		
P2P [25]	Diffusion	69.43	17.87	71.14	25.01	22.44	50	100
PnP [65]	Diffusion	28.22	22.28	79.05	25.41	22.55	50	100
PnP-Inv. [30]	Diffusion	24.29	22.46	79.68	25.41	22.62	50	100
EditFriendly [27]	Diffusion	-	24.55	81.57	23.97	21.03	50	100
MasaCtrl [11]	Diffusion	28.38	22.17	79.67	23.96	21.16	50	100
InfEdit [79]	Diffusion	<u>13.78</u>	<u>28.51</u>	85.66	25.03	22.22	12	72
RF-Inv. [52]	FLUX	40.60	20.82	71.92	25.20	22.11	28	56
RF-Solver [69]	FLUX	31.10	22.90	81.90	26.00	22.88	15	60
FireFlow [16]	FLUX	28.30	23.28	82.82	25.98	<u>22.94</u>	15	32
Ours (N = 15, $\alpha = 0.6$)	SD3	21.40	24.96	<u>86.11</u>	<u>26.39</u>	22.72	15	28
Ours (N = 15, $\alpha = 0.8$)	FLUX	26.85	24.10	84.86	26.97	23.51	15	37
Ours (N = 15, $\alpha = 0.6$)	FLUX	10.14	29.54	90.42	25.80	22.33	15	28

Table 2. **Text-driven image editing comparison** on PIE-Bench [30]. We report the peer-reviewed results of each baseline, and evaluate our proposed Uni-Edit using the relatively lightweight Stable Diffusion 3 (SD3) [19] and FLUX [32] to demonstrate the effectiveness. The best and second best results are **bolded** and underlined, respectively. Cells are highlighted from worse to better.

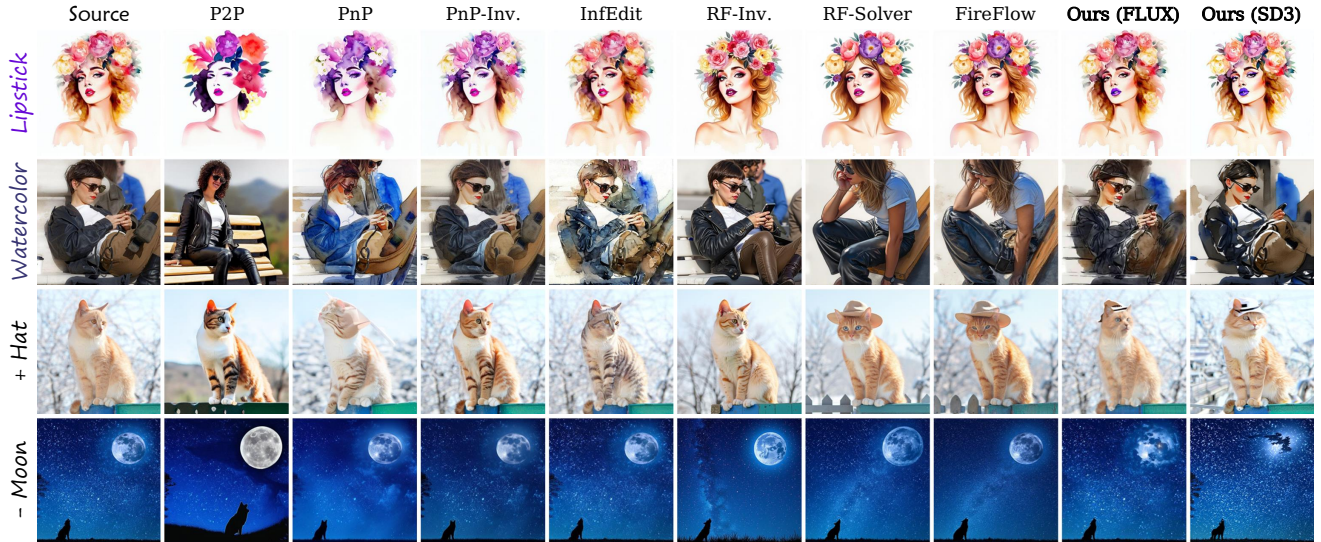


Figure 7. **Qualitative comparison on image editing.** Our method consistently achieves more appropriate editing with better background preservation across various flow models.

Bench [30], which contains 700 images with 10 different editing types. To evaluate edit-irrelevant context preservation, we use structure distance [64], along with PSNR and SSIM for annotated unedited regions. The performance of the edits is assessed using CLIP similarity [48] for both the whole image and the edited regions. More visualization and results are provided in the Appendix C, D, and F.

Implementation: We primarily conduct experiments using stable-diffusion-3-medium (SD3) [19] and FLUX.1-dev [32] models. For inversion and reconstruction, we set the sampling step to 50 for SD3 and 30 for FLUX, while for image editing, we use 15 steps with a delay rate α of 0.6 or 0.8. The relationship between the delay

rate and NFE is $NFE = 3\alpha N + 1$. The guidance strength ω is fixed at 5 for all experiments. Additional results of our method applied to diffusion models [44] and various datasets [28, 88] are provided in Appendix G.

5.2. Real Image Inversion & Reconstruction

Quantitative Comparison: Tab. 1 provides the quantitative results for reconstruction across various flow-based methods. We reconstruct images using only the inverted noise, without utilizing latent features from the inversion process. The results demonstrate that our proposed Uni-Inv consistently outperforms the baselines across different models and settings, including the unconditional case where



Figure 8. **Visualization of Uni-Edit process.** The guidance mask of each denoising step is shown at the upper right of the image. We also demonstrate the "Sphinx" phenomenon that existing latent fusion approaches may cause at the lower left of the figure.

text description is absent.

Qualitative Comparison: Fig. 6 shows the qualitative comparison of inversion and reconstruction across methods. Our method achieves nearly identical reconstruction results in both unconditional and conditional settings for various flow models. In contrast, other methods struggle with reconstruction without text conditions and show weaker performance even when image captions are available. These results strongly highlight the effectiveness of our Uni-Inv.

5.3. Text-driven Image Editing

Quantitative Comparison: Tab. 2 presents the quantitative results for text-driven image editing. Our method, Uni-Edit, consistently outperforms other approaches, particularly excelling in CLIP similarity. Based on SD3, Uni-Edit achieves a balance between background preservation and editing effectiveness, outperforming existing flow-based methods in both areas. On FLUX, it surpasses the inherent limitations of training-free approaches in background preservation while maintaining competitive editing performance. More results on diffusion models are given in Appendix E.

Qualitative Comparison: Fig. 7 compares the visual editing outcomes across methods. Attention-based approaches often transfer attributes to unrelated areas (e.g., P2P, PnP, and PnP-Inversion add purple to the overall image rather than focusing on specific regions, like lipstick). Sampling-based methods without regional constraints suffer from mis-edits or insufficient editing (e.g., RF-Solver and FireFlow). In contrast, our method provides precise guidance for both local modification and global stylization. Additional results on various datasets [28, 88] are provided in Appendix G.

Procedure Analysis: Fig. 8 visualizes the editing procedure. The superscript 0 indicates the result is directly transitioned from the sample to $t = 0$ using its current velocity. Early steps focus on broader areas with stronger editing intensity to eliminate original concepts, while later steps refine details, reducing the influence of m_i . We also show re-

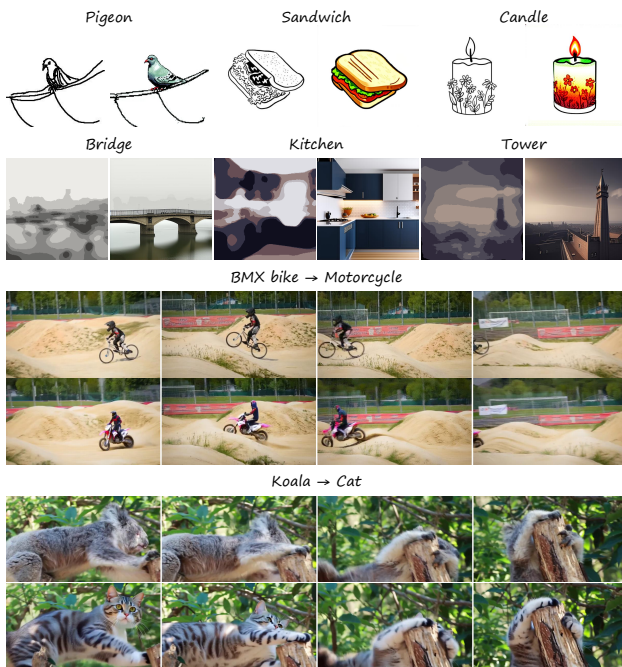


Figure 9. **Diverse application of Uni-Edit.** The top is sketch to image, and the bottom is stroke to image. The left of a image pair is the source image, and the right is the editing result.

sults from the existing latent fusion method [14, 24], which uses masks to fuse inversion and edit latents. These results lead to unnatural, "Sphinx"-like outputs, highlighting the adaptability and efficiency of our approach.

5.4. Applications

In addition to general text-driven image editing, the interpretable design of our method enables a wide range of applications. Fig. 9 showcases its use for sketch-to-image (1st line) and stroke-to-image (2nd line) tasks [12, 84]. For these applications, we set $\alpha = 0.8$ or 1 to enhance the editing effect. By exploiting the binary nature of sketches and fix-

ing m_i as their grayscale value, we achieve more robust results for sketch-to-image tasks. Moreover, thanks to the advanced flow matching-based video generation model Wan [73], we further test Uni-Edit on video editing tasks. We directly consider the latent containing the temporal dimension as Z , and apply Uni-Edit to Wan’s sampling process without any modification. Setting $\alpha = 0.8$ and $N = 25$, we achieve reliable editing results (3rd and 4th parts) using Wan2.1-T2V-1.3B model. These results further highlight the generalizability and effectiveness of our approach. More visualization results of video editing on videos from the DAVIS dataset [45] are provided in Appendix G.

6. Conclusion

We introduce a novel, tuning-free, model-agnostic methodology that combines the reconstruction-effective inversion method Uni-Inv with a region-aware, training-free image editing strategy Uni-Edit. To exploit the properties of flow models, we design robust, region-adaptive guidance in Uni-Edit to enhance the delayed injection framework, supported by Uni-Inv. Extensive experiments validate the effectiveness of our approach, demonstrating remarkable results while maintaining low inference costs. We will explore more diverse conditions (*e.g.*, adopt an image as a personalization prompt) that can be injected for further customized image editing in the future.

References

- [1] Michael S Albergo, Nicholas M Boffi, and Eric Vandenberg. Stochastic interpolants: A unifying framework for flows and diffusions. *arXiv preprint arXiv:2303.08797*, 2023. 3
- [2] Omri Avrahami, Dani Lischinski, and Ohad Fried. Blended diffusion for text-driven editing of natural images. In *Proceedings of the IEEE/CVF conference on computer vision and pattern recognition*, pages 18208–18218, 2022. 1, 2
- [3] Omri Avrahami, Ohad Fried, and Dani Lischinski. Blended latent diffusion. *ACM transactions on graphics (TOG)*, 42(4):1–11, 2023. 1
- [4] Omri Avrahami, Or Patashnik, Ohad Fried, Egor Nemchinov, Kfir Aberman, Dani Lischinski, and Daniel Cohen-Or. Stable flow: Vital layers for training-free image editing. *arXiv preprint arXiv:2411.14430*, 2024. 2
- [5] Lichen Bai, Shitong Shao, Zikai Zhou, Zipeng Qi, Zhiqiang Xu, Haoyi Xiong, and Zeke Xie. Zigzag diffusion sampling: Diffusion models can self-improve via self-reflection. In *The Thirteenth International Conference on Learning Representations*, 2024. 2
- [6] Omer Bar-Tal, Lior Yariv, Yaron Lipman, and Tali Dekel. Multidiffusion: Fusing diffusion paths for controlled image generation. 2023. 1
- [7] Manuel Brack, Felix Friedrich, Dominik Hintersdorf, Lukas Struppek, Patrick Schramowski, and Kristian Kersting. Sega: Instructing text-to-image models using semantic guidance. *Advances in Neural Information Processing Systems*, 36: 25365–25389, 2023. 2
- [8] Manuel Brack, Felix Friedrich, Katharia Kornmeier, Linoy Tsaban, Patrick Schramowski, Kristian Kersting, and Apolinário Passos. Ledits++: Limitless image editing using text-to-image models. In *Proceedings of the IEEE/CVF conference on computer vision and pattern recognition*, pages 8861–8870, 2024. 3
- [9] Arwen Bradley and Preetum Nakkiran. Classifier-free guidance is a predictor-corrector. *arXiv preprint arXiv:2408.09000*, 2024. 2
- [10] Tim Brooks, Aleksander Holynski, and Alexei A Efros. Instructpix2pix: Learning to follow image editing instructions. In *Proceedings of the IEEE/CVF conference on computer vision and pattern recognition*, pages 18392–18402, 2023. 6, 4
- [11] Mingdeng Cao, Xintao Wang, Zhongang Qi, Ying Shan, Xiaohu Qie, and Yinqiang Zheng. Masactrl: Tuning-free mutual self-attention control for consistent image synthesis and editing. In *Proceedings of the IEEE/CVF International Conference on Computer Vision (ICCV)*, pages 22560–22570, 2023. 3, 6, 7, 4
- [12] Pinaki Nath Chowdhury, Aneeshan Sain, Ayan Kumar Bhunia, Tao Xiang, Yulia Gryaditskaya, and Yi-Zhe Song. Fscoco: Towards understanding of freehand sketches of common objects in context. In *European conference on computer vision*, pages 253–270. Springer, 2022. 8
- [13] Hyungjin Chung, Jeongsol Kim, Michael T Mccann, Marc L Klasky, and Jong Chul Ye. Diffusion posterior sampling for general noisy inverse problems. *arXiv preprint arXiv:2209.14687*, 2022. 2
- [14] Guillaume Couairon, Jakob Verbeek, Holger Schwenk, and Matthieu Cord. Diffedit: Diffusion-based semantic image editing with mask guidance. *arXiv preprint arXiv:2210.11427*, 2022. 2, 3, 5, 6, 8
- [15] Yusuf Dalva, Kavana Venkatesh, and Pinar Yanardag. Fluxspace: Disentangled semantic editing in rectified flow transformers. *arXiv preprint arXiv:2412.09611*, 2024. 2
- [16] Yingying Deng, Xiangyu He, Changwang Mei, Peisong Wang, and Fan Tang. Fireflow: Fast inversion of rectified flow for image semantic editing, 2024. 2, 6, 7, 4
- [17] Yan Di, Chenyangguang Zhang, Pengyuan Wang, Guangyao Zhai, Ruida Zhang, Fabian Manhardt, Benjamin Busam, Xiangyang Ji, and Federico Tombari. Ccd-3dr: Consistent conditioning in diffusion for single-image 3d reconstruction. *arXiv preprint arXiv:2308.07837*, 2023. 1
- [18] Wenkai Dong, Song Xue, Xiaoyue Duan, and Shumin Han. Prompt tuning inversion for text-driven image editing using diffusion models. In *Proceedings of the IEEE/CVF International Conference on Computer Vision*, pages 7430–7440, 2023. 3
- [19] Patrick Esser, Sumith Kulal, Andreas Blattmann, Rahim Entezari, Jonas Müller, Harry Saini, Yam Levi, Dominik Lorenz, Axel Sauer, Frederic Boesel, et al. Scaling rectified flow transformers for high-resolution image synthesis. In *Forty-first international conference on machine learning*, 2024. 2, 3, 6, 7
- [20] Rinon Gal, Yuval Alaluf, Yuval Atzmon, Or Patashnik, Amit H Bermano, Gal Chechik, and Daniel Cohen-Or. An image is worth one word: Personalizing text-to-image generation using textual inversion. *arXiv preprint arXiv:2208.01618*, 2022. 1
- [21] Daniel Garibi, Or Patashnik, Andrey Voynov, Hadar Averbuch-Elor, and Daniel Cohen-Or. Renoise: Real image inversion through iterative noising, 2024. 2, 4, 6, 3
- [22] Ian Goodfellow, Jean Pouget-Abadie, Mehdi Mirza, Bing Xu, David Warde-Farley, Sherjil Ozair, Aaron Courville, and Yoshua Bengio. Generative adversarial networks. *Communications of the ACM*, 63(11):139–144, 2020. 2
- [23] Ligong Han, Song Wen, Qi Chen, Zhixing Zhang, Kunpeng Song, Mengwei Ren, Ruijiang Gao, Anastasis Sthopoulos, Xiaoxiao He, Yuxiao Chen, et al. Improving tuning-free real image editing with proximal guidance. *arXiv preprint arXiv:2306.05414*, 2023. 2
- [24] Ligong Han, Song Wen, Qi Chen, Zhixing Zhang, Kunpeng Song, Mengwei Ren, Ruijiang Gao, Anastasis Sthopoulos, Xiaoxiao He, Yuxiao Chen, et al. Proxedit: Improving tuning-free real image editing with proximal guidance. In *Proceedings of the IEEE/CVF Winter Conference on Applications of Computer Vision*, pages 4291–4301, 2024. 5, 6, 8
- [25] Amir Hertz, Ron Mokady, Jay Tenenbaum, Kfir Aberman, Yael Pritch, and Daniel Cohen-Or. Prompt-to-prompt image editing with cross attention control. *arXiv preprint arXiv:2208.01626*, 2022. 6, 7, 4

- [26] Jonathan Ho, Ajay Jain, and Pieter Abbeel. Denoising diffusion probabilistic models. *Advances in neural information processing systems*, 33:6840–6851, 2020. 1, 2
- [27] Inbar Huberman-Spiegelglas, Vladimir Kulikov, and Tomer Michaeli. An edit friendly ddpm noise space: Inversion and manipulations. In *Proceedings of the IEEE/CVF Conference on Computer Vision and Pattern Recognition*, pages 12469–12478, 2024. 3, 6, 7, 4
- [28] Mude Hui, Siwei Yang, Bingchen Zhao, Yichun Shi, Heng Wang, Peng Wang, Yuyin Zhou, and Cihang Xie. Hq-edit: A high-quality dataset for instruction-based image editing. *arXiv preprint arXiv:2404.09990*, 2024. 7, 8, 11
- [29] Quan Huynh-Thu and Mohammed Ghanbari. Scope of validity of psnr in image/video quality assessment. *Electronics letters*, 44(13):800–801, 2008. 6
- [30] Xuan Ju, Ailing Zeng, Yuxuan Bian, Shaoteng Liu, and Qiang Xu. Pnp inversion: Boosting diffusion-based editing with 3 lines of code. *International Conference on Learning Representations (ICLR)*, 2024. 2, 3, 6, 7, 4, 8, 9
- [31] Tero Karras, Samuli Laine, and Timo Aila. A style-based generator architecture for generative adversarial networks. In *Proceedings of the IEEE/CVF conference on computer vision and pattern recognition*, pages 4401–4410, 2019. 3
- [32] Black Forest Labs. Flux. <https://github.com/black-forest-labs/flux>, 2023. 6, 7
- [33] Black Forest Labs. Flux. <https://github.com/black-forest-labs/flux>, 2024. 2
- [34] Ziyi Li, Qinye Zhou, Xiaoyun Zhang, Ya Zhang, Yanfeng Wang, and Weidi Xie. Open-vocabulary object segmentation with diffusion models. In *Proceedings of the IEEE/CVF International Conference on Computer Vision*, pages 7667–7676, 2023. 1
- [35] Yaron Lipman, Ricky TQ Chen, Heli Ben-Hamu, Maximilian Nickel, and Matt Le. Flow matching for generative modeling. *arXiv preprint arXiv:2210.02747*, 2022. 3
- [36] Xingchao Liu, Chengyue Gong, and Qiang Liu. Flow straight and fast: Learning to generate and transfer data with rectified flow. *arXiv preprint arXiv:2209.03003*, 2022. 3, 4
- [37] Xingchao Liu, Xiwen Zhang, Jianzhu Ma, Jian Peng, et al. InstafLOW: One step is enough for high-quality diffusion-based text-to-image generation. In *The Twelfth International Conference on Learning Representations*, 2023. 3
- [38] Cheng Lu, Yuhao Zhou, Fan Bao, Jianfei Chen, Chongxuan Li, and Jun Zhu. Dpm-solver++: Fast solver for guided sampling of diffusion probabilistic models. *arXiv preprint arXiv:2211.01095*, 2022. 2
- [39] Ségolène Martin, Anne Gagneux, Paul Hagemann, and Gabriele Steidl. Pnp-flow: Plug-and-play image restoration with flow matching. *arXiv preprint arXiv:2410.02423*, 2024. 3
- [40] Ron Mokady, Amir Hertz, Kfir Aberman, Yael Pritch, and Daniel Cohen-Or. Null-text inversion for editing real images using guided diffusion models. In *Proceedings of the IEEE/CVF conference on computer vision and pattern recognition*, pages 6038–6047, 2023. 2, 6, 3, 4
- [41] Gaurav Parmar, Krishna Kumar Singh, Richard Zhang, Yijun Li, Jingwan Lu, and Jun-Yan Zhu. Zero-shot image-to-image translation. In *ACM SIGGRAPH 2023 Conference Proceedings, SIGGRAPH 2023, Los Angeles, CA, USA, August 6-10, 2023*, pages 11:1–11:11. ACM, 2023. 3, 4
- [42] Maitreya Patel, Song Wen, Dimitris N. Metaxas, and Yezhou Yang. Steering rectified flow models in the vector field for controlled image generation. *arXiv preprint arXiv:2412.00100*, 2024. 3
- [43] William Peebles and Saining Xie. Scalable diffusion models with transformers. In *Proceedings of the IEEE/CVF international conference on computer vision*, pages 4195–4205, 2023. 1, 2
- [44] Dustin Podell, Zion English, Kyle Lacey, Andreas Blattmann, Tim Dockhorn, Jonas Müller, Joe Penna, and Robin Rombach. Sdxl: Improving latent diffusion models for high-resolution image synthesis. *arXiv preprint arXiv:2307.01952*, 2023. 7, 3, 4
- [45] Jordi Pont-Tuset, Federico Perazzi, Sergi Caelles, Pablo Arbeláez, Alexander Sorkine-Hornung, and Luc Van Gool. The 2017 davis challenge on video object segmentation. *arXiv:1704.00675*, 2017. 9, 12
- [46] Ben Poole, Ajay Jain, Jonathan T Barron, and Ben Mildenhall. Dreamfusion: Text-to-3d using 2d diffusion. *arXiv preprint arXiv:2209.14988*, 2022. 1
- [47] Qi Qian, Haiyang Xu, Ming Yan, and Juhua Hu. Siminversion: A simple framework for inversion-based text-to-image editing. *arXiv preprint arXiv:2409.10476*, 2024. 2
- [48] Alec Radford, Jong Wook Kim, Chris Hallacy, Aditya Ramesh, Gabriel Goh, Sandhini Agarwal, Girish Sastry, Amanda Askell, Pamela Mishkin, Jack Clark, et al. Learning transferable visual models from natural language supervision. In *International conference on machine learning*, pages 8748–8763. PMLR, 2021. 7
- [49] Aditya Ramesh, Prafulla Dhariwal, Alex Nichol, Casey Chu, and Mark Chen. Hierarchical text-conditional image generation with clip latents. *arXiv preprint arXiv:2204.06125*, 1(2):3, 2022. 1
- [50] Jiawei Ren, Liang Pan, Jiayang Tang, Chi Zhang, Ang Cao, Gang Zeng, and Ziwei Liu. Dreamgaussian4d: Generative 4d gaussian splatting. *arXiv preprint arXiv:2312.17142*, 2023. 1
- [51] Robin Rombach, Andreas Blattmann, Dominik Lorenz, Patrick Esser, and Björn Ommer. High-resolution image synthesis with latent diffusion models. In *Proceedings of the IEEE/CVF conference on computer vision and pattern recognition*, pages 10684–10695, 2022. 1
- [52] Litu Rout, Yujia Chen, Nataniel Ruiz, Constantine Caramanis, Sanjay Shakkottai, and Wen-Sheng Chu. Semantic image inversion and editing using rectified stochastic differential equations. *arXiv preprint arXiv:2410.10792*, 2024. 2, 7, 4
- [53] Nataniel Ruiz, Yuanzhen Li, Varun Jampani, Yael Pritch, Michael Rubinstein, and Kfir Aberman. Dreambooth: Fine tuning text-to-image diffusion models for subject-driven generation. 2022. 1
- [54] Mohammad Shahab Sefehri, Zalan Fabian, Maryam Soltanolkotabi, and Mahdi Soltanolkotabi. Mediconfusion: Can you trust your ai radiologist? probing the reliability

- of multimodal medical foundation models. *arXiv preprint arXiv:2409.15477*, 2024. 1
- [55] Piyush Sharma, Nan Ding, Sebastian Goodman, and Radu Soricut. Conceptual captions: A cleaned, hypernymed, image alt-text dataset for automatic image captioning. In *Proceedings of ACL*, 2018. 6, 5
- [56] Yichun Shi, Peng Wang, and Weilin Huang. Seedit: Align image re-generation to image editing. *arXiv preprint arXiv:2411.06686*, 2024. 6, 4
- [57] Saurabh Singh and Ian Fischer. Stochastic sampling from deterministic flow models. *arXiv preprint arXiv:2410.02217*, 2024. 2
- [58] Jiaming Song, Chenlin Meng, and Stefano Ermon. Denoising diffusion implicit models. *arXiv preprint arXiv:2010.02502*, 2020. 2, 4
- [59] Kaiyu Song and Hanjiang Lai. Leveraging previous steps: A training-free fast solver for flow diffusion. *arXiv preprint arXiv:2411.07627*, 2024. 2
- [60] Yang Song, Jascha Sohl-Dickstein, Diederik P Kingma, Abhishek Kumar, Stefano Ermon, and Ben Poole. Score-based generative modeling through stochastic differential equations. *arXiv preprint arXiv:2011.13456*, 2020. 2, 4
- [61] Zhicheng Sun, Zhenhao Yang, Yang Jin, Haozhe Chi, Kun Xu, Liwei Chen, Hao Jiang, Yang Song, Kun Gai, and Yadong Mu. Rectifid: Personalizing rectified flow with anchored classifier guidance. *Advances in Neural Information Processing Systems*, 37:96993–97026, 2024. 3
- [62] Jiayang Tang, Jiawei Ren, Hang Zhou, Ziwei Liu, and Gang Zeng. Dreamgaussian: Generative gaussian splatting for efficient 3d content creation. *arXiv preprint arXiv:2309.16653*, 2023. 1
- [63] Linoy Tsaban and Apolinário Passos. Ledits: Real image editing with ddpm inversion and semantic guidance. *arXiv preprint arXiv:2307.00522*, 2023. 3
- [64] Narek Tumanyan, Omer Bar-Tal, Shai Bagon, and Tali Dekel. Splicing vit features for semantic appearance transfer. In *Proceedings of the IEEE/CVF Conference on Computer Vision and Pattern Recognition*, pages 10748–10757, 2022. 7
- [65] Narek Tumanyan, Michal Geyer, Shai Bagon, and Tali Dekel. Plug-and-play diffusion features for text-driven image-to-image translation. In *IEEE/CVF Conference on Computer Vision and Pattern Recognition, CVPR 2023, Vancouver, BC, Canada, June 17-24, 2023*, pages 1921–1930. IEEE, 2023. 2, 6, 7, 4
- [66] Bram Wallace, Akash Gokul, and Nikhil Naik. Edict: Exact diffusion inversion via coupled transformations. In *Proceedings of the IEEE/CVF Conference on Computer Vision and Pattern Recognition*, pages 22532–22541, 2023. 2
- [67] Fangyikang Wang, Hubery Yin, Yue-Jiang Dong, Huminhao Zhu, Hanbin Zhao, Hui Qian, Chen Li, et al. Belm: Bidirectional explicit linear multi-step sampler for exact inversion in diffusion models. *Advances in Neural Information Processing Systems*, 37:46118–46159, 2025. 2
- [68] Fu-Yun Wang, Ling Yang, Zhaoyang Huang, Mengdi Wang, and Hongsheng Li. Rectified diffusion: Straightness is not your need in rectified flow. *arXiv preprint arXiv:2410.07303*, 2024. 2
- [69] Jiangshan Wang, Junfu Pu, Zhongang Qi, Jiayi Guo, Yue Ma, Nisha Huang, Yuxin Chen, Xiu Li, and Ying Shan. Taming rectified flow for inversion and editing. *arXiv preprint arXiv:2411.04746*, 2024. 2, 6, 7, 4
- [70] Kuan-Chieh Wang, Daniil Ostashev, Yuwei Fang, Sergey Tulyakov, and Kfir Aberman. Moa: Mixture-of-attention for subject-context disentanglement in personalized image generation. In *SIGGRAPH Asia 2024 Conference Papers*, pages 1–12, 2024. 1
- [71] Qian Wang, Biao Zhang, Michael Birsak, and Peter Wonka. Mdp: A generalized framework for text-guided image editing by manipulating the diffusion path. *arXiv preprint arXiv:2303.16765*, 2023. 3
- [72] Zhou Wang, Alan C Bovik, Hamid R Sheikh, and Eero P Simoncelli. Image quality assessment: from error visibility to structural similarity. *IEEE transactions on image processing*, 13(4):600–612, 2004. 6
- [73] WanTeam, Ang Wang, Baole Ai, Bin Wen, Chaojie Mao, Chen-Wei Xie, Di Chen, Feiwu Yu, Haiming Zhao, Jianxiao Yang, Jianyuan Zeng, Jiayu Wang, Jingfeng Zhang, Jingen Zhou, Jinkai Wang, Jixuan Chen, Kai Zhu, Kang Zhao, Keyu Yan, Lianghua Huang, Mengyang Feng, Ningyi Zhang, Pandeng Li, Pingyu Wu, Ruihang Chu, Ruili Feng, Shiwei Zhang, Siyang Sun, Tao Fang, Tianxing Wang, Tianyi Gui, Tingyu Weng, Tong Shen, Wei Lin, Wei Wang, Wei Wang, Wenmeng Zhou, Wenten Wang, Wenting Shen, Wenyuan Yu, Xianzhong Shi, Xiaoming Huang, Xin Xu, Yan Kou, Yangyu Lv, Yifei Li, Yijing Liu, Yiming Wang, Yingya Zhang, Yitong Huang, Yong Li, You Wu, Yu Liu, Yulin Pan, Yun Zheng, Yuntao Hong, Yupeng Shi, Yutong Feng, Zeyinzi Jiang, Zhen Han, Zhi-Fan Wu, and Ziyu Liu. Wan: Open and advanced large-scale video generative models. *arXiv preprint arXiv:2503.20314*, 2025. 9, 7
- [74] Cong Wei, Zheyang Xiong, Weiming Ren, Xinrun Du, Ge Zhang, and Wenhua Chen. Omniedit: Building image editing generalist models through specialist supervision. *arXiv preprint arXiv:2411.07199*, 2024. 6, 4
- [75] Chen Henry Wu and Fernando De la Torre. A latent space of stochastic diffusion models for zero-shot image editing and guidance. In *Proceedings of the IEEE/CVF International Conference on Computer Vision*, pages 7378–7387, 2023. 3
- [76] Qiucheng Wu, Yujian Liu, Handong Zhao, Ajinkya Kale, Trung Bui, Tong Yu, Zhe Lin, Yang Zhang, and Shiyu Chang. Uncovering the disentanglement capability in text-to-image diffusion models. In *Proceedings of the IEEE/CVF conference on computer vision and pattern recognition*, pages 1900–1910, 2023. 3
- [77] Zongze Wu, Nicholas Kolkin, Jonathan Brandt, Richard Zhang, and Eli Shechtman. Turboedit: Instant text-based image editing. In *European Conference on Computer Vision*, pages 365–381. Springer, 2024. 6, 4
- [78] Guangxuan Xiao, Tianwei Yin, William T Freeman, Frédo Durand, and Song Han. Fastcomposer: Tuning-free multi-subject image generation with localized attention. *International Journal of Computer Vision*, pages 1–20, 2024. 3
- [79] Sihan Xu, Yidong Huang, Jiayi Pan, Ziqiao Ma, and Joyce Chai. Inversion-free image editing with natural language. 2024. 3, 6, 7, 4

- [80] Yu Xu, Fan Tang, Juan Cao, Yuxin Zhang, Xiaoyu Kong, Jintao Li, Oliver Deussen, and Tong-Yee Lee. Head-router: A training-free image editing framework for mm-dits by adaptively routing attention heads. *arXiv preprint arXiv:2411.15034*, 2024. [2](#)
- [81] Hu Ye, Jun Zhang, Sibao Liu, Xiao Han, and Wei Yang. Ip-adapter: Text compatible image prompt adapter for text-to-image diffusion models. *arXiv preprint arXiv:2308.06721*, 2023. [1](#)
- [82] Taoran Yi, Jiemin Fang, Junjie Wang, Guanjun Wu, Lingxi Xie, Xiaopeng Zhang, Wenyu Liu, Qi Tian, and Xinggang Wang. Gaussiandreamer: Fast generation from text to 3d gaussians by bridging 2d and 3d diffusion models. In *Proceedings of the IEEE/CVF Conference on Computer Vision and Pattern Recognition*, pages 6796–6807, 2024. [1](#)
- [83] Haonan Yin, Guanlong Jiao, Qianhui Wu, Borje F Karlsson, Biqing Huang, and Chin Yew Lin. Lafite: Latent diffusion model with feature editing for unsupervised multi-class anomaly detection. *arXiv preprint arXiv:2307.08059*, 2023. [1](#)
- [84] Fisher Yu, Ari Seff, Yinda Zhang, Shuran Song, Thomas Funkhouser, and Jianxiong Xiao. Lsun: Construction of a large-scale image dataset using deep learning with humans in the loop. *arXiv preprint arXiv:1506.03365*, 2015. [8](#)
- [85] Guoqiang Zhang, Jonathan P Lewis, and W Bastiaan Kleijn. Exact diffusion inversion via bidirectional integration approximation. In *European Conference on Computer Vision*, pages 19–36. Springer, 2024. [2](#)
- [86] Lvmin Zhang, Anyi Rao, and Maneesh Agrawala. Adding conditional control to text-to-image diffusion models. In *Proceedings of the IEEE/CVF international conference on computer vision*, pages 3836–3847, 2023. [1](#)
- [87] Richard Zhang, Phillip Isola, Alexei A Efros, Eli Shechtman, and Oliver Wang. The unreasonable effectiveness of deep features as a perceptual metric. In *Proceedings of the IEEE conference on computer vision and pattern recognition*, pages 586–595, 2018. [6](#)
- [88] Haozhe Zhao, Xiaojian Ma, Liang Chen, Shuzheng Si, Rujie Wu, Kaikai An, Peiyu Yu, Minjia Zhang, Qing Li, and Baobao Chang. Ultraedit: Instruction-based fine-grained image editing at scale, 2024. [7](#), [8](#), [10](#)
- [89] Jun-Yan Zhu, Taesung Park, Phillip Isola, and Alexei A Efros. Unpaired image-to-image translation using cycle-consistent adversarial networkss. In *Computer Vision (ICCV), 2017 IEEE International Conference on*, 2017. [3](#)

UNEDIT-FLOW: Unleashing Inversion and Editing in the Era of Flow Models

Supplementary Material

A. Proof of Proposition 4.1

Prop. 4.1: Suppose the velocity field \mathbf{v}_θ is Lipschitz, and there is a constant C such that $\|\mathbf{Z}_{t_p} - \mathbf{Z}_{t_q}\| \leq C \|t_p - t_q\|$, $\forall t_p, t_q \in [0, 1]$, where \mathbf{Z}_{t_p} and \mathbf{Z}_{t_q} come from the same sampling process. Then for any two consecutive steps t_{i-1} and t_i , the local error of inversion and reconstruction using Uni-Inv is $\mathcal{O}(\Delta t_i^3)$, where $\Delta t_i = t_i - t_{i-1}$.

Assumption 1. The velocity function $\mathbf{v}_\theta(\cdot, \tau)$ is X_1 -Lipschitz for $\forall \tau \in [0, 1]$, i.e., given a τ , $\|\mathbf{v}_\theta(\zeta_1, \tau) - \mathbf{v}_\theta(\zeta_2, \tau)\| \leq X_1 \|\zeta_1 - \zeta_2\|$ for $\forall \zeta_1, \zeta_2$.

Assumption 2. The velocity function $\mathbf{v}_\theta(\zeta, \cdot)$ is X_2 -Lipschitz for $\forall \zeta$, i.e., given a ζ , $\|\mathbf{v}_\theta(\zeta, \tau_1) - \mathbf{v}_\theta(\zeta, \tau_2)\| \leq X_2 \|\tau_1 - \tau_2\|$ for $\forall \tau_1, \tau_2$.

Assumption 3. $\|\mathbf{Z}_{t_p} - \mathbf{Z}_{t_q}\| \leq C \|t_p - t_q\|$, $\forall p, q \in [0, 1]$ when \mathbf{Z}_{t_p} and \mathbf{Z}_{t_q} come from the same trajectory.

Proof. Given a deterministic solver, e.g. Euler's method:

$$\mathbf{Z}_{t_{i-1}} = \mathbf{Z}_{t_i} + (t_{i-1} - t_i) \mathbf{v}_\theta(\mathbf{Z}_{t_i}, t_i). \quad (\text{A.1})$$

The corresponding inversion step of Uni-Inv is denoted by:

$$\widehat{\mathbf{Z}}_{t_i} = \widehat{\mathbf{Z}}_{t_{i-1}} - (t_{i-1} - t_i) \widehat{\mathbf{v}}_i, \quad (\text{A.2})$$

where $\widehat{\mathbf{v}}_i$ is obtained via Algo. 1 and can be expressed as:

$$\widehat{\mathbf{v}}_i = \mathbf{v}_\theta\left(\widehat{\mathbf{Z}}_{t_{i-1}} - (t_{i-1} - t_i) \bar{\mathbf{v}}_{i-1}, t_i\right). \quad (\text{A.3})$$

Define the estimation error \mathcal{E}_i as $\mathcal{E}_i = \|\mathbf{Z}_{t_i} - \widehat{\mathbf{Z}}_{t_i}\|$. Bringing Eq. A.1 and Eq. A.2 into it, we obtain that:

$$\mathcal{E}_i = (t_{i-1} - t_i) \|\widehat{\mathbf{v}}_i - \mathbf{v}_\theta(\mathbf{Z}_{t_i}, t_i)\|. \quad (\text{A.4})$$

Denote $\mathcal{E}_i^1 = \|\widehat{\mathbf{v}}_i - \mathbf{v}_\theta(\mathbf{Z}_{t_i}, t_i)\|$, we can bring in Eq. A.3:

$$\mathcal{E}_i^1 = \left\| \mathbf{v}_\theta\left(\widehat{\mathbf{Z}}_{t_{i-1}} - (t_{i-1} - t_i) \bar{\mathbf{v}}_{i-1}, t_i\right) - \mathbf{v}_\theta(\mathbf{Z}_{t_i}, t_i) \right\|. \quad (\text{A.5})$$

Using the Lipschitz continuity of $\mathbf{v}_\theta(\cdot, \tau)$, we have:

$$\mathcal{E}_i^1 \leq X_1 \left\| \widehat{\mathbf{Z}}_{t_{i-1}} - (t_{i-1} - t_i) \bar{\mathbf{v}}_{i-1} - \mathbf{Z}_{t_i} \right\|. \quad (\text{A.6})$$

Bring in Eq. A.1 for \mathbf{Z}_{t_i} , there is:

$$\begin{aligned} \mathcal{E}_i^1 &\leq X_1 \left\| \left(\widehat{\mathbf{Z}}_{t_{i-1}} - \mathbf{Z}_{t_{i-1}} \right) + \right. \\ &\quad \left. (t_{i-1} - t_i) (\mathbf{v}_\theta(\mathbf{Z}_{t_i}, t_i) - \bar{\mathbf{v}}_{i-1}) \right\| \\ &\leq X_1 \left\| \widehat{\mathbf{Z}}_{t_{i-1}} - \mathbf{Z}_{t_{i-1}} \right\| + \\ &\quad X_1 (t_{i-1} - t_i) \|\mathbf{v}_\theta(\mathbf{Z}_{t_i}, t_i) - \bar{\mathbf{v}}_{i-1}\|. \end{aligned} \quad (\text{A.7})$$

The first term is the accumulative error of the previous steps. We denote it as $\mathcal{E}_i^A = \left\| \widehat{\mathbf{Z}}_{t_{i-1}} - \mathbf{Z}_{t_{i-1}} \right\|$ and it should be neglected for local error analysis. We further denote $\mathcal{E}_i^2 = \|\mathbf{v}_\theta(\mathbf{Z}_{t_i}, t_i) - \bar{\mathbf{v}}_{i-1}\|$. To analyse this item, we first consider a second-order case, i.e., utilizing an additional function evaluation step to calculate $\bar{\mathbf{v}}_{i-1} = \mathbf{v}_\theta(\widehat{\mathbf{Z}}_{t_{i-1}}, t_{i-1})$. Then we have:

$$\mathcal{E}_i^2 = \left\| \mathbf{v}_\theta(\mathbf{Z}_{t_i}, t_i) - \mathbf{v}_\theta(\widehat{\mathbf{Z}}_{t_{i-1}}, t_{i-1}) \right\|. \quad (\text{A.8})$$

Using the Lipschitz continuity of $\mathbf{v}_\theta(\cdot, \tau)$ and $\mathbf{v}_\theta(\zeta, \cdot)$, we have:

$$\begin{aligned} \mathcal{E}_i^2 &= \left\| \mathbf{v}_\theta(\mathbf{Z}_{t_i}, t_i) - \mathbf{v}_\theta(\mathbf{Z}_{t_i}, t_{i-1}) + \right. \\ &\quad \left. \mathbf{v}_\theta(\mathbf{Z}_{t_i}, t_{i-1}) - \mathbf{v}_\theta(\widehat{\mathbf{Z}}_{t_{i-1}}, t_{i-1}) \right\| \\ &\leq \|\mathbf{v}_\theta(\mathbf{Z}_{t_i}, t_i) - \mathbf{v}_\theta(\mathbf{Z}_{t_i}, t_{i-1})\| + \\ &\quad \left\| \mathbf{v}_\theta(\mathbf{Z}_{t_i}, t_{i-1}) - \mathbf{v}_\theta(\widehat{\mathbf{Z}}_{t_{i-1}}, t_{i-1}) \right\| \\ &\leq X_1 \left\| \mathbf{Z}_{t_i} - \widehat{\mathbf{Z}}_{t_{i-1}} \right\| + X_2 \|t_i - t_{i-1}\|. \end{aligned} \quad (\text{A.9})$$

We denote $\Delta t_i = t_i - t_{i-1}$. Using the Assumption 3, we have:

$$\begin{aligned} \mathcal{E}_i^2 &\leq X_1 \left(\left\| \mathbf{Z}_{t_i} - \mathbf{Z}_{t_{i-1}} \right\| + \left\| \mathbf{Z}_{t_{i-1}} - \widehat{\mathbf{Z}}_{t_{i-1}} \right\| \right) + X_2 \Delta t_i \\ &\leq (CX_1 + X_2) \Delta t_i + X_1 \mathcal{E}_i^A. \end{aligned} \quad (\text{A.10})$$

Ultimately, the estimation error is as follows:

$$\begin{aligned} \mathcal{E}_i &\leq \Delta t_i \mathcal{E}_i^1 \leq \Delta t_i (X_1 \mathcal{E}_i^A + X_1 \Delta t_i \mathcal{E}_i^2) \\ &\leq \Delta t_i (X_1 \mathcal{E}_i^A + X_1 \Delta t_i ((CX_1 + X_2) \Delta t_i + X_1 \mathcal{E}_i^A)) \\ &= X_1 (CX_1 + X_2) \Delta t_i^3 + (X_1^2 \Delta t_i^2 + X_1 \Delta t_i) \mathcal{E}_i^A. \end{aligned} \quad (\text{A.11})$$

For local error analysis, we neglect the global accumulated error \mathcal{E}_i^A , then we have the local error \mathcal{E}_i^L :

$$\mathcal{E}_i^L \leq X_1 (CX_1 + X_2) \Delta t_i^3 = \mathcal{O}(\Delta t_i^3). \quad (\text{A.12})$$

Furthermore, since the step count of the iterative algorithm is $\mathcal{O}(1/\Delta t_i)$, we can have the global error: $\mathcal{E}^G = \mathcal{O}\left(\max_i (\Delta t_i^2)\right)$.

Now, let's go back to the second-order case assumption $\bar{\mathbf{v}}_{i-1} = \mathbf{v}_\theta(\widehat{\mathbf{Z}}_{t_{i-1}}, t_{i-1})$ we mentioned earlier. From a

practical perspective, Algo. 1 provides an additional function evaluation in the initialization stage, making its first step the standard second-order case. After that, in the ideal case, each \bar{v}_i should converge to v_i , and thus the first-order approximation of the algorithm does not significantly affect the error. Theoretically, since that:

$$\begin{aligned}\bar{v}_{i-1} &= v_\theta(\bar{Z}_{i-1}, t_{i-1}), \\ \bar{Z}_{i-1} &= \hat{Z}_{i-2} - (t_{i-2} - t_{i-1})\bar{v}_{i-2},\end{aligned}\quad (\text{A.13})$$

neglecting the last-step accumulated error, we can derive that

$$\|\hat{Z}_{i-1} - \bar{Z}_{i-1}\| \leq \Delta t_{i-1} \|\hat{v}_{i-2} - \bar{v}_{i-2}\|. \quad (\text{A.14})$$

Using the Lipschitz continuity of $v_\theta(\cdot, \tau)$, we can get:

$$\|\hat{v}_{i-2} - \bar{v}_{i-2}\| \leq X_1 \|\hat{Z}_{i-2} - \bar{Z}_{i-2}\|. \quad (\text{A.15})$$

Neglecting the last-step accumulated error of velocity estimation for local error calculation, we note that the one-order approximation brings no change to the conclusion of $\mathcal{E}_i^L = \mathcal{O}(\Delta t_i^3)$.

This local error serves the dual processes of inversion and reconstruction, theoretically ensuring the effectiveness of our proposed inversion in practical applications. Moreover, our approach does not utilize the derivative approximation to achieve the result, only expects the velocity function to have good mathematical properties.

B. Theoretical Analysis of Uni-Edit

Conducting a mathematical perspective, our proposed Uni-Edit can be compressed into a single arithmetic representation. As shown in Algo. 2, we have the editing result:

$$\begin{aligned}\tilde{Z}_{t_{i-1}} &= \tilde{Z}_{t_i} + (t_{i-1} - t_i) v_i^F \\ &= \tilde{Z}_{t_i} + \mathbf{s}_i + (t_{i-1} - t_i) v_i^F \\ &= \tilde{Z}_{t_i} + \omega(t_{i-1} - t_i)(\mathbf{1} + \mathbf{m}_i) \odot (v_i^T - v_i^S) \\ &\quad + (t_{i-1} - t_i)(\mathbf{m}_i \odot v_i^T + (\mathbf{1} - \mathbf{m}_i) \odot v_i^S) \\ &= \tilde{Z}_{t_i} + (t_{i-1} - t_i) v_i^*,\end{aligned}\quad (\text{B.16})$$

and the reformed velocity is:

$$\begin{aligned}v_i^* &= \omega(\mathbf{1} + \mathbf{m}_i) \odot (v_i^T - v_i^S) + \\ &\quad (\mathbf{m}_i \odot v_i^T + (\mathbf{1} - \mathbf{m}_i) \odot v_i^S) \\ &= v_i^S + (\omega(\mathbf{1} + \mathbf{m}_i) + \mathbf{m}_i) \odot (v_i^T - v_i^S),\end{aligned}\quad (\text{B.17})$$

It's interesting that we finally obtain a velocity v_i^* which is very similar to the classifier-free guidance (CFG) [13] but with a per-pixel-variant weight instead of a single constant

value. Some previous works consider CFG as a predictor-corrector [9, 58]. From this perspective, whereas we take a different yet more interpretable approach to conduct a predictor-corrector, and eventually obtain a method with adaptive guidance strength for different regions. In the manuscript, we experimentally validate that the mask obtained from our designed sampling strategy is rationally adaptive to vary with the editing objective and the iteration step. Therefore, our method ensures to achieve per-pixel adaptive guidance strength within the framework of predictor-corrector, which in turn confers effectiveness for text-driven image editing to flow models.

C. Ablation Studies of Uni-Edit

In Fig. C.1, we present the ablation studies of our proposed Uni-Edit with step = 15 for various hyper-parameters. The results demonstrate that different hyper-parameters bring rational skews to the trade-off between background preservation and editing effectiveness. Nevertheless, our approach improves the overall level of the trade-off, making it effortless to bring benefits for both aspects.

D. Uni-Inv on Different Generation Methods

D.1. Heun Method based Uni-Inv

To validate the transferability and effectiveness of our method on different samplers, we reimplement our Uni-Inv based on the Heun method. To be specific, since the Heun method is formulated as:

$$\begin{aligned}Z_{t_{i-1}} &= Z_{t_i} + \\ &\quad (t_{i-1} - t_i) \frac{v_\theta(Z_{t_i}, t_i) + v_\theta(v_\theta(Z_{t_i}, t_i), t_i)}{2},\end{aligned}\quad (\text{D.18})$$

we directly reform the velocity function as:

$$v_\theta^H(\zeta, \tau) = \frac{v_\theta(\zeta, \tau) + v_\theta(v_\theta(\zeta, \tau), \tau)}{2}, \quad (\text{D.19})$$

then using v_θ^H to replace the original velocity function in Algo. 1. As shown in Tab. D.1, our approach improves the reconstruction accuracy of the Heun method across the board. This demonstrates the flexibility and adaptability of Uni-Inv to different samplers and reflects its effectiveness.

D.2. DDIM based Uni-Inv

DDIM [58] provides an efficient sampling method for the stochastic-differential-equation-based diffusion models and allows access to the sampling strategy with the form of ordinary differential equations. Benefiting from this, we are able to migrate Uni-Inv to diffusion models by simply treating the predicted initial noise as a velocity, utilizing the cached last-step predicted noise to push forward the current samples to the next timestep, thus performing

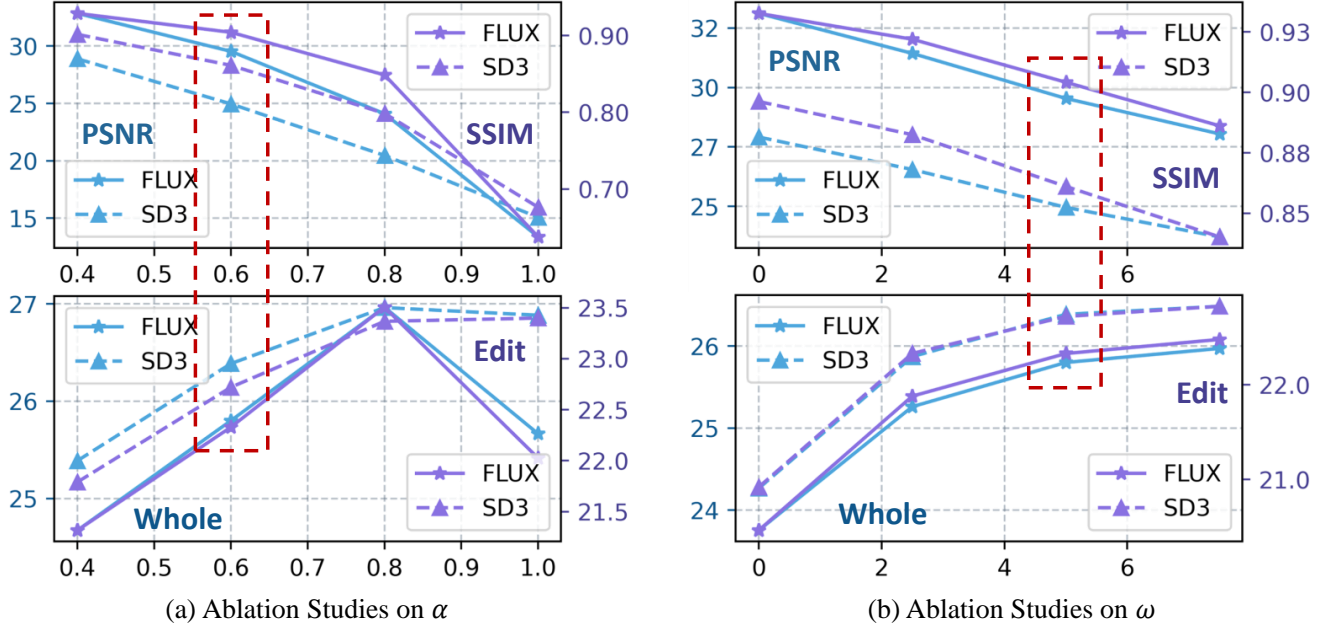


Figure C.1. **Ablation studies of Uni-Edit** on (a) delay rate α and (b) guidance strength ω . The top indicates the background preservation, while the bottom refers to CLIP scores of editing.

Method	Model	Unconditional				Conditional			
		$MSE_{10^3}^{\downarrow}$	$PSNR^{\uparrow}$	$SSIM_{10^2}^{\uparrow}$	$LPIPS_{10^2}^{\downarrow}$	$MSE_{10^3}^{\downarrow}$	$PSNR^{\uparrow}$	$SSIM_{10^2}^{\uparrow}$	$LPIPS_{10^2}^{\downarrow}$
DDIM	SDXL	8.99	22.19	75.57	12.76	7.35	23.21	77.73	10.20
Ours (DDIM)		6.32	24.18	79.05	8.60	5.17	25.04	80.63	6.95
Heun	SD3	25.34	16.98	67.25	26.63	26.32	16.89	64.14	27.70
Ours (Heun)		20.23	20.10	76.38	15.76	12.75	22.31	79.62	12.43
Heun	FLUX	83.04	11.77	42.10	39.96	76.79	12.17	40.17	41.18
Ours (Heun)		57.39	13.63	57.45	26.95	32.35	16.79	67.33	21.25

Table D.1. **Quantitative results for inversion and reconstruction** of our Uni-Inv based on Heun method with Flow models and DDIM with Diffusion models. We set the step to 50 for SDXL [44], 25 for SD3 [19], and 15 for FLUX models to conduct the experiments. The best results are **bolded**.

our inversion. We evaluate the above strategy on SDXL (RealVisXL.V4.0) [44]. The results are shown in Tab. D.1. Though DDIM has already demonstrated strong feasibility in numerous applications, our approach can still take it to the next level and bring about an overall improvement in reconstruction accuracy. It also indicates that our work does not just face a particular methodology. We expect to build approaches that can continuously provide insights into the developing trend of generative models.

E. Uni-Edit on Diffusion Models

Similar to Uni-Inv, since our proposed Uni-Edit is completely sample-based and model-agnostic, it is also capable of migrating to diffusion models effortlessly. We adopt

the SDXL (RealVisXL.V4.0) [44] as our base model, conducting evaluation experiments on PIE-Bench [30]. The results are shown in Tab. E.2. Here we enumerate the previous SOTA of diffusion-based approaches, wherein compared to the manuscript, we additionally present the results of tuning-based inversion [21, 40] applied to editing. In contrast to these approaches, the CLIP similarity metrics exemplify our proposed Uni-Edit’s capability to drive the diffusion-based editing to new heights and maintain highly competitive background preservation. Meanwhile, we significantly improve the editing efficiency by reducing NFE extremely compared to previous diffusion-based approaches. These experiments demonstrate strongly the effectiveness, adaptability, and generalizability of our pro-

Method	Model	Structure	BG Preservation		CLIP Sim.↑		Steps	NFE
		Distance \downarrow_{10^3}	PSNR \uparrow	SSIM \uparrow_{10^2}	Whole	Edited		
Null-Text Inv [40]	Diffusion	13.44	27.03	84.11	24.75	21.86	50	-
ReNoise [21]	Diffusion	-	27.11	72.30	23.98	21.26	50	-
P2P [25]	Diffusion	69.43	17.87	71.14	25.01	22.44	50	100
P2P-Zero [41]	Diffusion	61.68	20.44	74.67	22.80	20.54	50	100
PnP [65]	Diffusion	28.22	22.28	79.05	<u>25.41</u>	22.55	50	100
PnP-Inv. [30]	Diffusion	24.29	22.46	79.68	<u>25.41</u>	<u>22.62</u>	50	100
EditFriendly [27]	Diffusion	-	24.55	81.57	23.97	21.03	50	100
MasaCtrl [11]	Diffusion	28.38	22.17	79.67	23.96	21.16	50	100
InfEdit [79]	Diffusion	13.78	28.51	85.66	25.03	22.22	12	72
Ours	Diffusion	<u>15.59</u>	<u>25.64</u>	<u>83.42</u>	26.33	22.78	15	28

Table E.2. **Text-driven image editing comparison** on PIE-Bench [30] based on Diffusion models. We evaluate our proposed Uni-Edit using SDXL [44]. We keep the same hyper-parameter setting with our main experiments (*i.e.*, $\alpha = 0.6$ and $\omega = 5$), and adopt 50 and 15 as steps. Besides tuning-based methods are marked in gray, the best and second best results are **bolded** and underlined, respectively.

posed approaches, providing new insights into image inversion and editing in the era of flow models.

Furthermore, there are still many training-based methods [10, 56, 74, 77] to learn how to reasonably edit images from the provided training data. Most of them focus on conducting flexible editing through user-provided instructions. Such ideas are very practical and effective. Nonetheless, before embarking on this kind of approach, it is crucial to clearly learn about the properties of the base generation methods. This is also the main concentration of this paper.

F. Additional Qualitative Comparison

F.1. Uni-Inv

We represent more qualitative comparison results of our Uni-Inv and recent flow-based approaches [16, 69] in Fig. F.2 and Fig. F.3. These figures contain a wide variety of image samples, including landscape photographs, object photographs, human-centered daily photographs, photographs in extreme lighting, group photographs of large numbers of people, black and white photographs, posters, pencil drawings, oil paintings, etc. of varying resolutions. Our method well maintains the overall image color (last line of Fig. F.2), texture style (6th line of Fig. F.2), content details including text (8th and 9th lines of Fig. F.3) during inversion & reconstruction, achieving consistent superiority in both conditional and unconditional settings.

F.2. Uni-Edit

We further perform additional qualitative comparisons with existing state-of-the-art methods [11, 16, 25, 27, 30, 52, 65, 69, 79] on text-driven image editing as shown in Fig. F.4, Fig. F.5, and Fig. F.6. We extensively compared the different approaches under conditions of editing categories, mate-

rials, properties, motions, backgrounds, and types of adding or removing items or concepts, as well as stylization.

First, in the task of regional editing, our method demonstrates significant local perception and background preservation capabilities. It is worth noting that our approach is model-agnostic, *i.e.* it does not require the involvement of the attention mechanism. This leads to more oriented regional editing. For example, attention-based methods such as PnP [65] often impose attributes that need to be used for regional editing on irrelevant regions (4th line of Fig. F.5). Due to these methods disassembling prompts and attempting to utilize a single token about the editing to exert guidance, inappropriate semantic understanding comes since the wholeness of prompts is destroyed. On the contrary, our approach is model-agnostic, thus better capitalizing on the text comprehension capabilities learned from the model.

Subsequently, compared to the same sampling-based kind of approaches (*i.e.*, RF-Inversion [52], RF-Solver [69], and FireFlow [16]), our method demonstrates significant advantages in terms of image structure and background preservation while maintaining robust editing (1st and 9th lines of Fig. F.4, 3rd and last lines of Fig. F.5, 3rd and 7th lines of Fig. F.6). On the one hand, this is due to our proposed Uni-Inv theoretically ensuring a small local error in the inversion process that can support accurate reconstruction. On the other hand, our deep exploration and re-empowerment of delayed injection make it easy for our proposed Uni-Edit to strike a satisfying balance between editing and the preservation of editing-irrelevant concepts.

G. Additional Results on Editing Tasks

Fig. G.7 and Fig. G.8 represent additional qualitative results of our proposed Uni-Edit on image editing tasks.

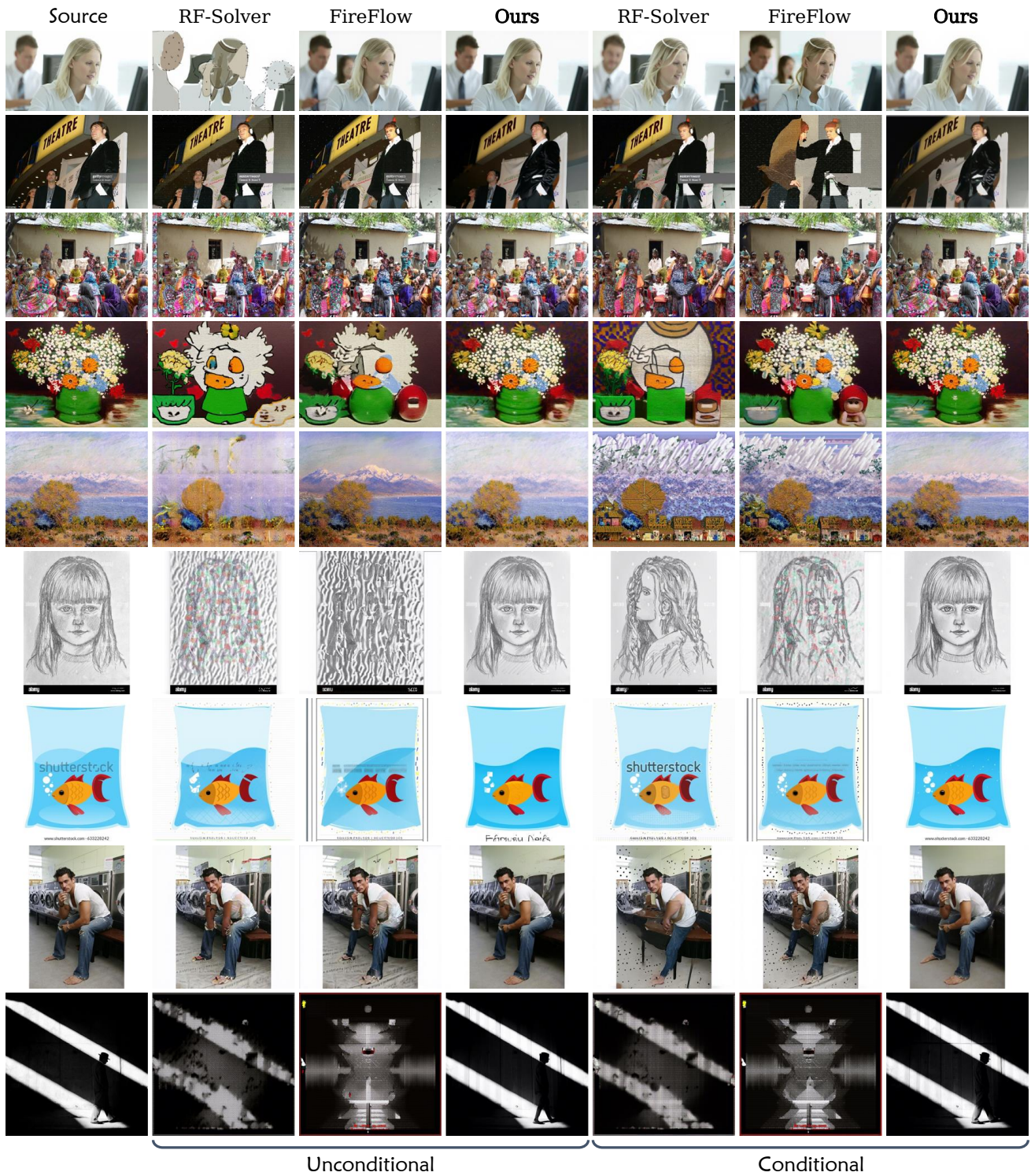


Figure F.2. **Additional qualitative comparison on inversion & reconstruction** on the Conceptual Captions validation dataset [55].

These results indicate that when it comes to diverse targets and diverse image domains, our approach still remains very effective. It is worth noting that each edit in Fig. G.7

contains multiple different editing objectives (e.g., changing the time, removing the crowd, and adjusting the lighting). Our approach is able to simultaneously achieve these

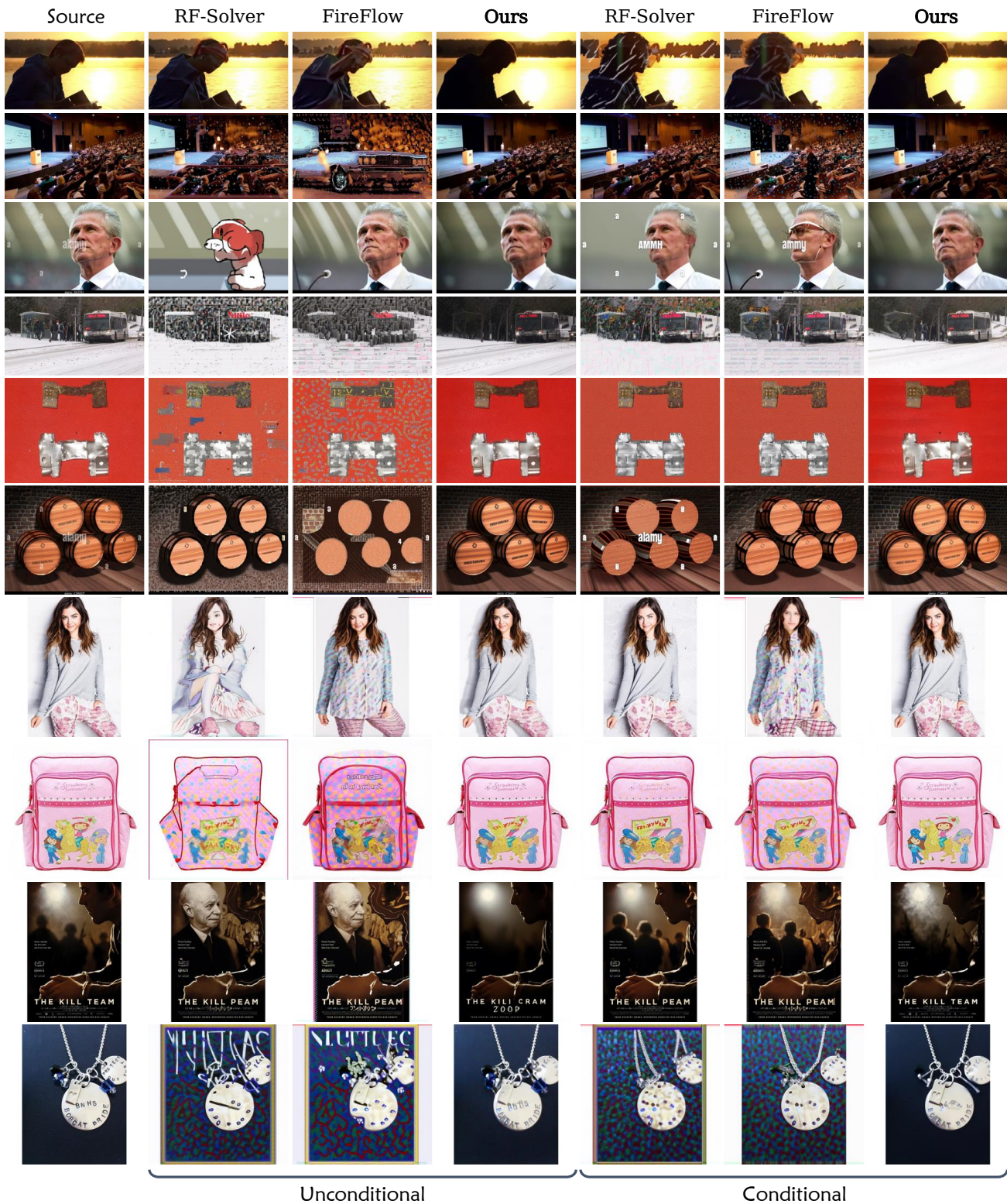


Figure F.3. Additional qualitative comparison on inversion & reconstruction on the Conceptual Captions validation dataset [55].

various targets in a single round, using only the original prompt and the target prompt as guidance. Benefiting from

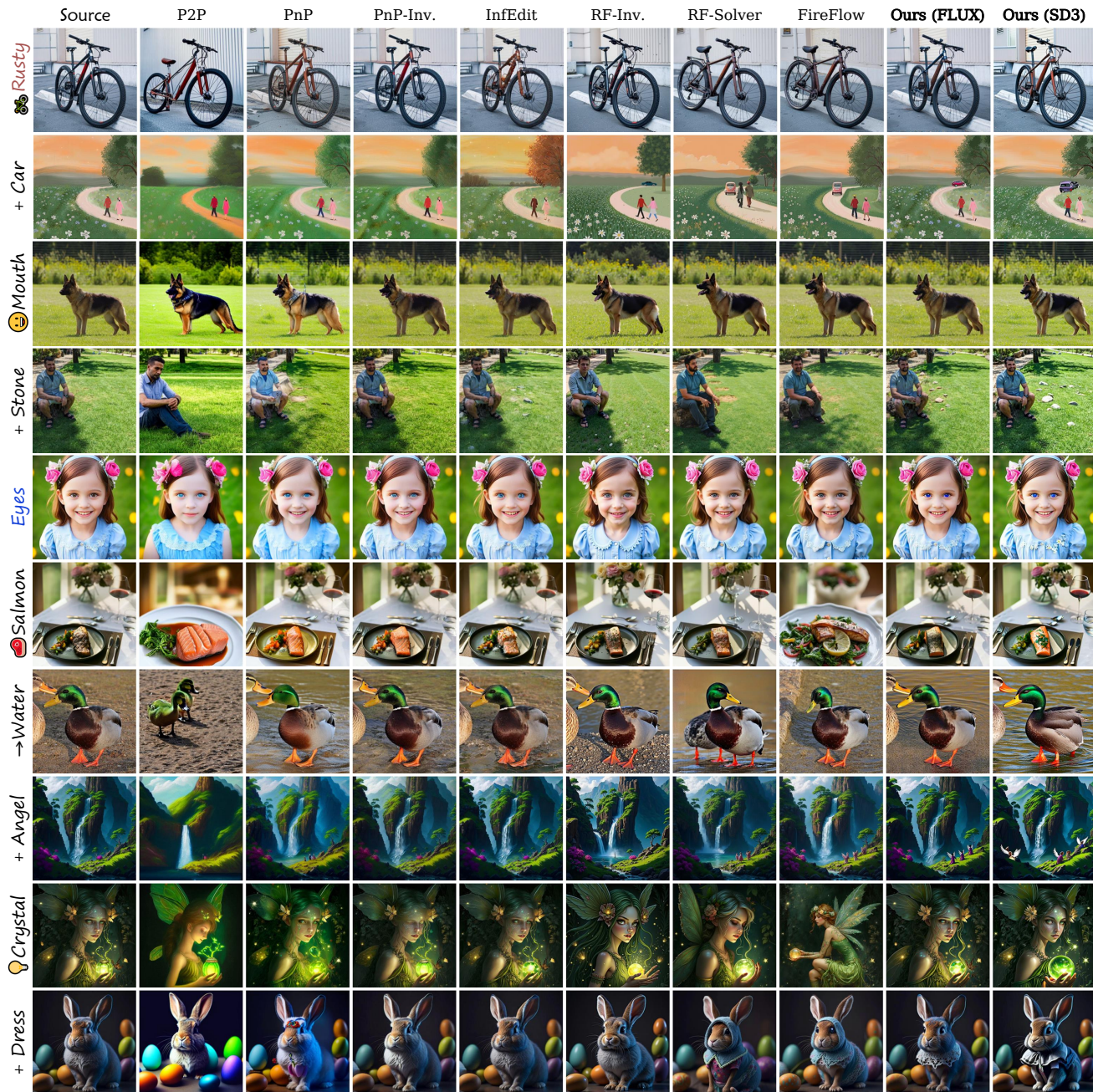


Figure F.4. Additional qualitative comparison on image editing on PIE-Bench [30].

the sampling-based design, our approach is able to capture diverse objectives at once through the relationship between the latents obtained from different conditions. Compared to methods that rely on cross attention manipulations, this design is simpler, more robust, and less likely to cause confusion.

Moreover, we directly adopt Uni-Edit to conduct video editing tasks using the flow matching-based video generation model Wan [73]. Qualitative results are shown in Fig.

G.9. Since our method is model-agnostic, we can achieve reliable video editing results without additional design or complex parameterization. This is further strong evidence of our approach’s generalizability.

H. Limitations and Future Works

The core issue plaguing us now is that our Uni-Edit is designed for image-text pair inputs. It is not capable of ac-

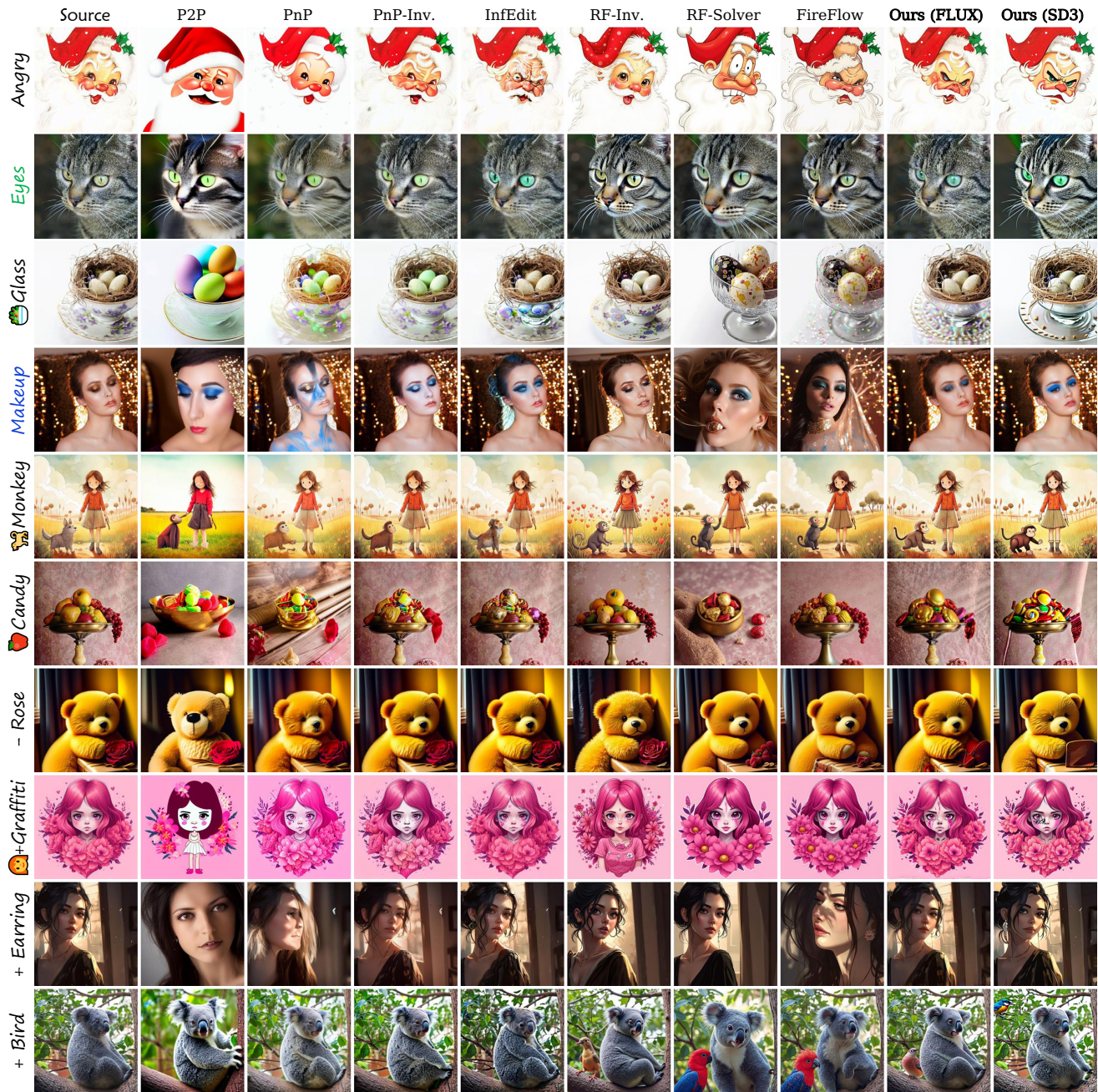


Figure F.5. Additional qualitative comparison on image editing on PIE-Bench [30].

cepting more than one image as the condition. This results in no direct way for us to contribute to the personalization generation problems. In the future, we would like to develop editing methods that are more general and oriented to more diverse tasks. The accurate inversion of Uni-Inv helps to capture image information. With this facilitation, we hope to develop sampling-based editing strategies capable of injecting image conditions based on our re-enabled delayed injection framework. We leave it as an interesting

future work.



Figure F.6. Additional qualitative comparison on image editing on PIE-Bench [30].

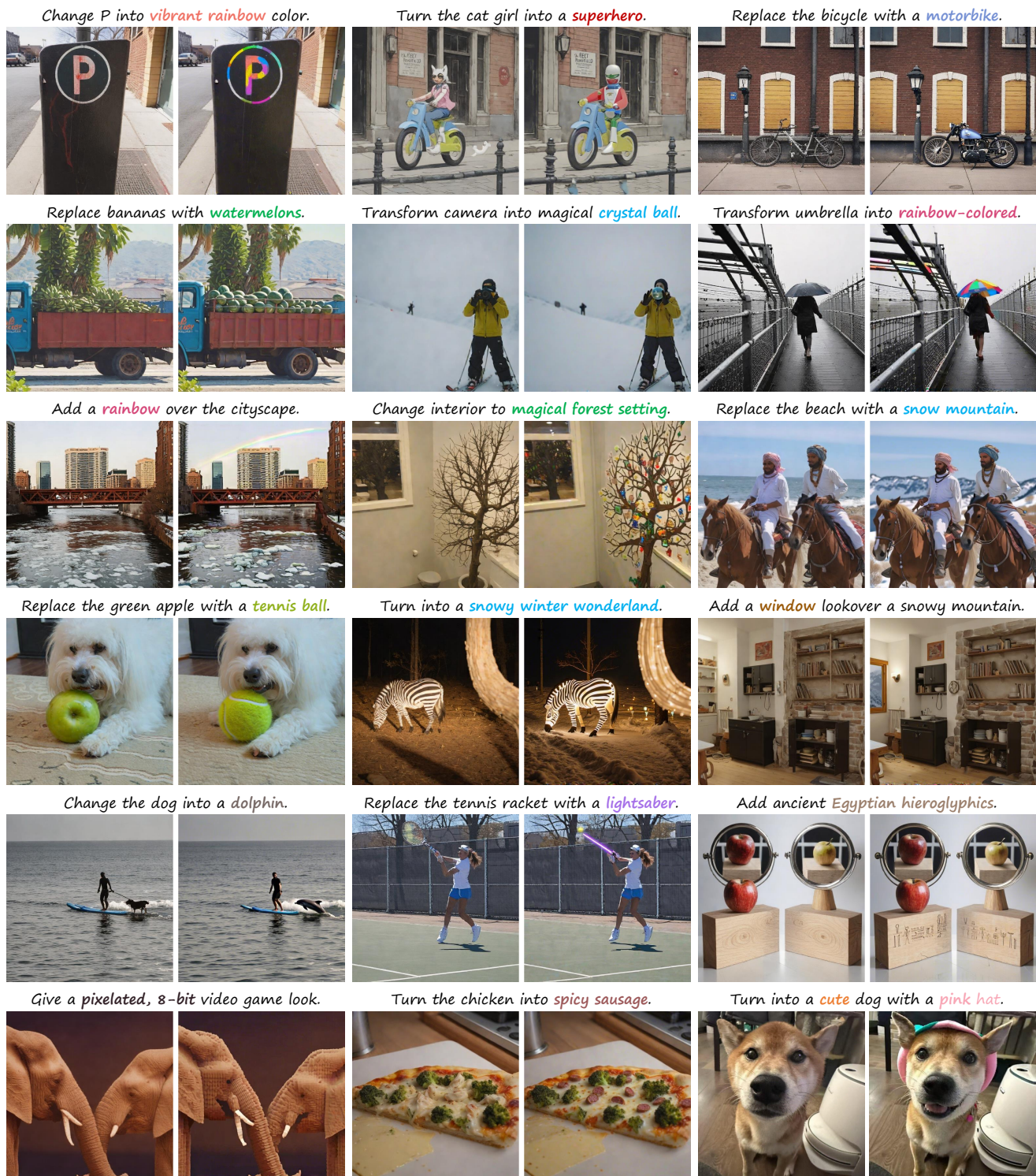


Figure G.7. **Additional qualitative results on image editing** on UltraEdit dataset [88] and wild images. In each image pair, the left is the original image and the right is the result of our editing. The text captions at the top of images are descriptions of the editing objectives and are not the input to the model. We still maintain the paradigm of using the original prompt and the target prompt as conditions. These images are obtained by FLUX using Uni-Edit with $\alpha = 0.6$, $\omega = 5$ and $\text{step} = 15$ which is consistent with the main experiments.

Remove the rust from the hammer, polish the metal to a shine, and replace the worn handle with a new wooden one.



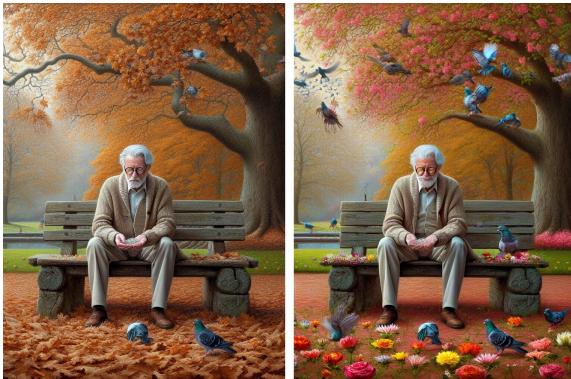
Colorize the sketch and add transform it into a life-like oil painting.



Transform the cat into a mechanical version with glowing blue eyes.



Change the season to spring by adding blooming flowers on the ground and on the trees, and increase the number of pigeons and add more flying in the sky.



Transform the cottage into a half-timbered house with white walls and dark wooden beams. Replace the landscape with vibrant cherry blossoms in full bloom.



Change the time of day to night, remove the crowd to make the market appear closed, and adjust the lighting to reflect a quieter atmosphere.



Change the weather to a dramatic storm with dark, swirling clouds and multiple lightning strikes hitting the sea.



Remove the engraving on the gold name tag.



Change the reflection on the teapot to show a clear blue sky with clouds instead of the bright kitchen window.



Figure G.8. Additional qualitative results on image editing on HQ-Edit dataset [28]. The visualization setup is the same as Fig. G.7.

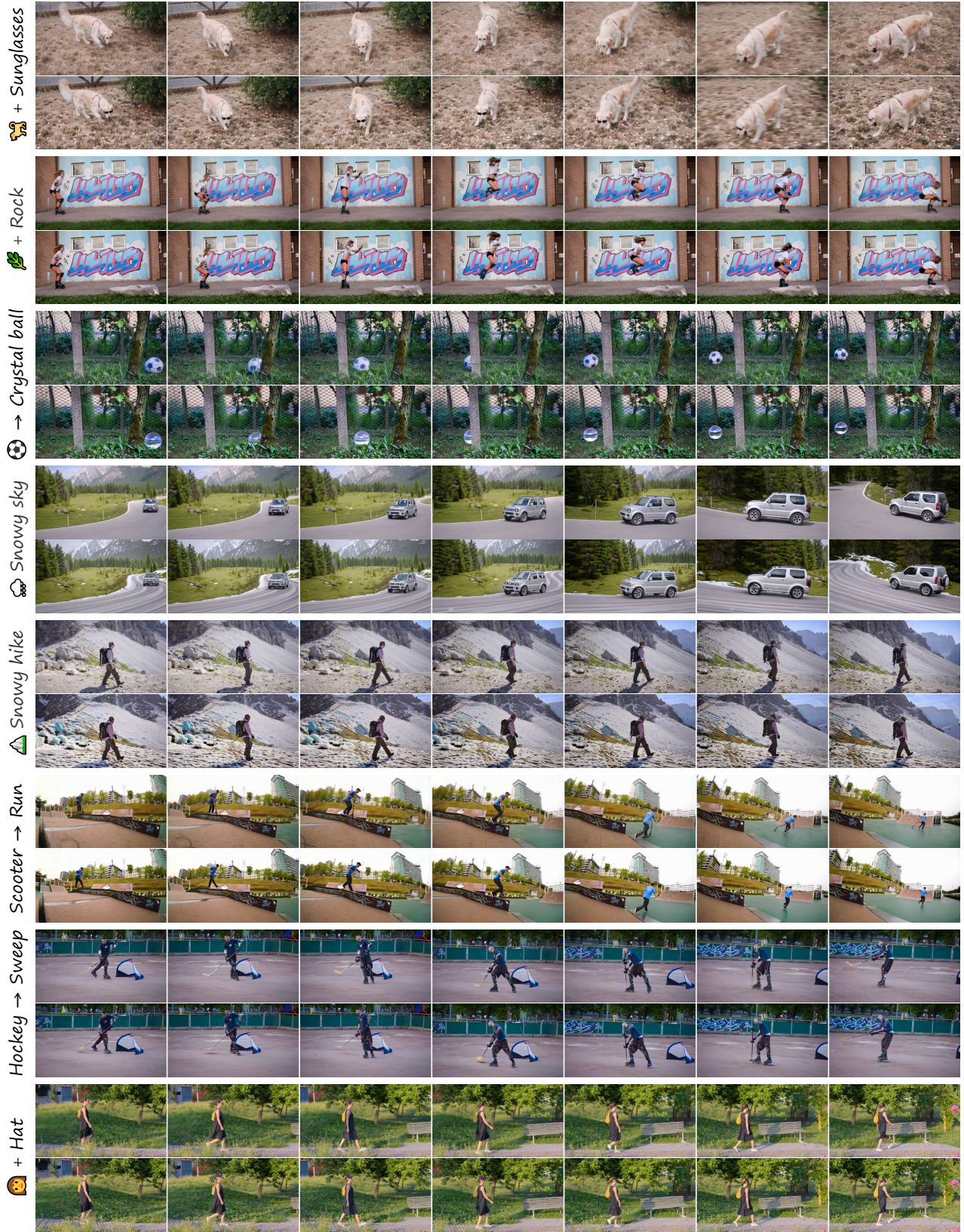


Figure G.9. Additional qualitative results on video editing on DAVIS dataset [45]. We set $\alpha = 0.8$, $\omega = 5$, $N = 25$ for the experiments.